

# 1

## Molecular Modeling in Mineralogy and Geochemistry

**Randall T. Cygan**

*Geochemistry Department  
Sandia National Laboratories  
Albuquerque, New Mexico, 87185-0750, U.S.A.*

*“A theory is something nobody believes, except the person who made it.  
An experiment is something everybody believes, except the person who made it.”*  
Attributed to Albert Einstein

*“A theory has only the alternative of being right or wrong.  
A model has a third possibility: it may be right, but irrelevant.”*  
Manfred Eigen

### INTRODUCTION

At what underlying fundamental level of understanding does geosciences research need to attain in order to evaluate the complex processes that control the weathering rate of silicate minerals? To investigate the formation of ore deposits and oil reservoirs, or the leaching of mine tailings into watersheds and the eventual contamination of groundwater? To predict the crustal deformation of long-term underground waste storage sites, or the stability of lower mantle phases and their effect on seismic signals? Or, for that matter, to examine tectonic uplift and cooling rates associated with orogenies? These and numerous other examples from mineralogy and geochemistry often require an understanding of atomic-level processes to identify the fundamental properties and mechanisms that control the thermodynamics and kinetics of Earth materials. Molecular models are often invoked to supplement field observations, experimental measurements, and spectroscopy. Theoretical methods provide a powerful complement for the experimentalist, especially with recent trends in which atomic-scale measurements are being made at synchrotron and other high-energy source facilities throughout the world. Such analytical methods and facilities have matured to such an extent that mineralogists and geochemists routinely probe Earth materials to evaluate bulk, surface, defect, intergranular, compositional, isotopic, long-range, local, order-disorder, electronic, and magnetic structures. Molecular modeling theory provides a means to help interpret the field and experimental observation, and to discriminate among various competing models to explain the macroscopic observation. And ultimately, molecular modeling provides the basis for prediction to further test the validity of the scientific hypothesis. This is especially significant in the geosciences where the conditions in the interior of the Earth, and other planets, preclude observation or are not achievable through experiment.

The explosion of computer technology and the development of faster processors and efficient algorithms have led to the development of specialized molecular modeling tools for computational chemistry. Combined with user-friendly interfaces and the porting of molecular modeling codes to personal computer platforms, these tools are increasingly being used by non-specialists to help interpret experimental and field observations. These tools are no longer limited to a specialized few who can understand the complex logic of thousands or millions of lines of software code, or those having access to government or university supercomputers. Commercial molecular modeling software is available to most researchers and is being used to examine an ever-increasing number mineralogical and geochemical problems. But what level of theory is required to best examine and solve a

particular problem? Can the problem even be solved on a personal computer, a Unix workstation, or does the researcher need a massively-parallel supercomputer? What is the theory, what are the limits of the various modeling methods, and how does one apply these modeling tools to the complex nature of Earth materials? These are the critical concerns addressed by this book.

The quote noted above and attributed to Albert Einstein describes the natural skepticism that might exist in linking experimental (or field) observations to molecular models. Experimentalists and theoreticians as members of their own research specialty will have a natural tendency to be misjudged by others. The inherent heterogeneous nature and complexity of the geosciences makes the connection between observation and theory even more complicated, yet numerous successes in other scientific disciplines, such as pharmaceuticals and materials science, have made molecular simulation an accepted approach. The critical success of molecular modeling and computer simulation in solving mineralogical and geochemical problems will ultimately be judged by the entire geosciences community.

### Historical perspective

Modern molecular modeling technology combines the most sophisticated and efficient, graphical-based software with a variety of computer platforms ranging from personal computers (and even hand-held devices) to massively-parallel supercomputers. The last decade has seen the most dramatic improvement in our ability to visualize structural models of molecules and periodic systems. Interestingly, it was not more than ten years ago that almost every introductory chemistry and mineralogy class required students to manipulate physical ball-and-stick models of molecules and crystals to help visualize and understand the structure and arrangement of atoms. In fact, for almost two hundred years this was *de rigueur* for most chemists. John Dalton, the founder of atomic theory, first introduced the concept of a molecular model in 1810 with his use of wooden balls connected by sticks to describe molecules (Rouvray 1995). Previously in 1808, the English chemist William Wollaston used hand-drawn sketches of atoms to visualize the tetrahedral coordination about a central atom (Rouvray 1997).

The Dutch chemist Jacobus van't Hoff built upon these early models by developing the first set of structural models for organic compounds based on the tetrahedral arrangement of hydrogens and other chemical groups about a central carbon atom. This work helped to explain the nature of organic isomers and optical activity that had confused chemists at that time (van't Hoff 1874). Further advances in the development of molecular modeling were led by the series of scientific breakthroughs in the late nineteenth and early twentieth century. These include the discovery of the electron in 1897 by the English physicist J. J. Thompson, and the development by Neils Bohr and Ernest Rutherford in 1911-1912 of an atomic model comprised of quantized electrons orbiting around a dense nucleus. In 1924, the French physicist Louis de Broglie recognized the wave-particle duality of matter that ultimately led to the 1926 publication of the famous wavefunction equation ( $H\psi=E\psi$ ) by the physicist Erwin Schrödinger. The quantum description of many-electron chemical systems was developed in the 1930's by the efforts of Douglas Hartree and Vladimir Fock using an exact Hamiltonian and approximate wavefunctions. Refinements on the use of electronic structure calculations were later introduced by Kohn and Sham (1965) and by Hehre et al. (1969). Ultimately, these pioneering efforts in quantum chemistry methods led to the awarding of the Nobel Prize for chemistry in 1998 to Walter Kohn for developing density functional methods and John Pople for developing molecular orbital theory.

The structural analysis of molecular systems, especially proteins and other

macromolecules, was of significant interest starting in the mid-twentieth century primarily due to the advances in crystallographic and spectroscopic methods. Physical molecular models needed to visualize large biochemical molecules were introduced by Robert Corey, Linus Pauling, Walter Koltun, and Andre Dreiding in the 1950's and 1960's. Kendrew et al. (1958) published the first three dimensional model of a protein (myoglobin) based on X-ray analysis and a wire-mesh representation of the structure. Advances in computer technology in the 1960's brought computer visualization to the forefront of biochemistry and aided in the analysis of protein structure and protein folding (Levinthal 1966). The trend increased through the 1970's and 1980's as the drug industry recognized the usefulness of computer visualization methods to help design new pharmaceuticals and organic molecules.

The modern era of molecular modeling probably began with the introduction of empirical-based energy forcefields, such as the one developed by Lifson and Warshel (1968), to assist with the conformational and configuration analysis of simple organic compounds. Computationally-fast energy calculations (as opposed to costly quantum methods) could now be performed on a large number of molecular configurations allowing one to determine the lowest energy structures (i.e., the most stable). Combining these molecular mechanics approaches with the interactive visualization provided by fast graphical computer displays allowed molecular modeling to quickly expand in the 1990's. Calculations involving inorganic compounds, including a good number of mineral phases, were not performed using molecular mechanics methods until the 1970's and 1980's. William Busing, Richard Catlow, and Leslie Woodcock (e.g., Busing 1970; Catlow et al. 1976; Woodcock et al. 1976; Catlow et al. 1982) pioneered much of the early work associated with the simulation of oxides and silicate minerals. The use of quantum methods in mineralogy was being done at the same time, with much credit going to the pioneering studies of Gerald Gibbs and John Tossell (e.g., Gibbs et al. 1972; Tossell and Gibbs 1977, 1978; Gibbs 1982).

### Molecular modeling tools

In general, computer simulation techniques cover a broad range of spatial and temporal variation. This is best demonstrated in the schematic diagram presented in Figure 1. Modeling geologic-scale processes pushes the distance and time scales to even larger values. Traditional continuum and finite element methods of simulation often reach

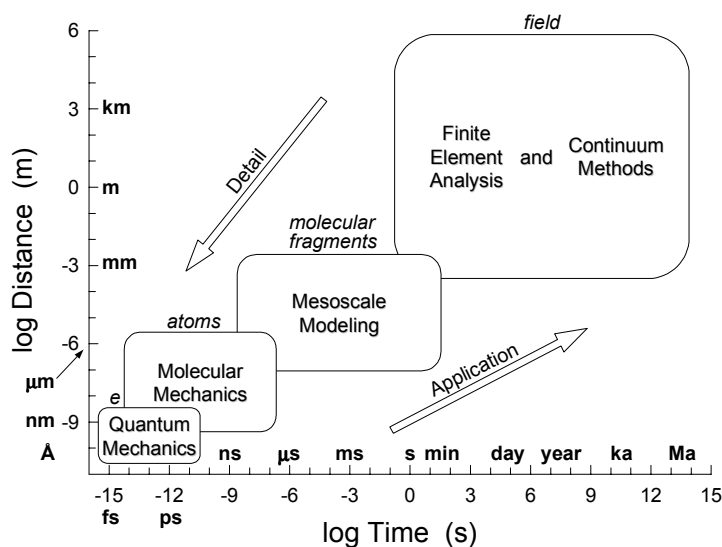


**Figure 1.** Schematic representation of the various computer simulation methods as a function of spatial and temporal variables. Boundaries between methods are approximate and diffuse to represent overlap of the techniques.

to kilometer (field scale) or greater length scales and times involving millions of years (geological times). In contrast, molecular modeling methods fall at the opposite extreme where distances are typically on the order of Ångstroms (level of atomic separations) and times are on the order of femtoseconds (time scale of molecular vibrations). The transition between these two modeling extremes includes the analysis of electrons for quantum chemistry, atoms for molecular mechanics models, molecular fragments for mesoscale models, and macroscopic units for the larger-scale field models. Although the boundaries in this representation are in practice quite diffuse and significant overlap of the techniques occurs, each method provides the necessary detail for the respective scale of the modeling. Obviously, there is a greater span of scales needed to link molecular models to the large scale geological applications in the upper right of the diagram. Mesoscale modeling methods are not discussed in this book, but several recent reviews and examples of the various techniques are available (e.g., Stockman et al. 1997; Coles et al. 1998; Flekkoy and Coveney 1999).

There are several excellent handbooks and texts that provide comprehensive reviews of molecular modeling methods. Noteworthy among these are Clark (1985) and Allen and Tildesley (1987), and the more recent volumes by Frenkel and Smit (1996) and Leach (1996). The recent publication by Schleyer (1998) presents an outstanding and thorough review of computational chemistry including numerous, and almost exhaustive, discussions of theory, methods, forcefields, and software. However, the significant size (five volumes and over three thousand pages) and associative cost may prevent any practical access to the information.

Molecular modeling tools concentrate, in general, on calculating the total energy of the molecular or periodic system under investigation. Two fundamental approaches are typically used in this effort: molecular mechanics and quantum mechanics. Figure 2 provides a schematic representation and flow chart of how these methods are related and

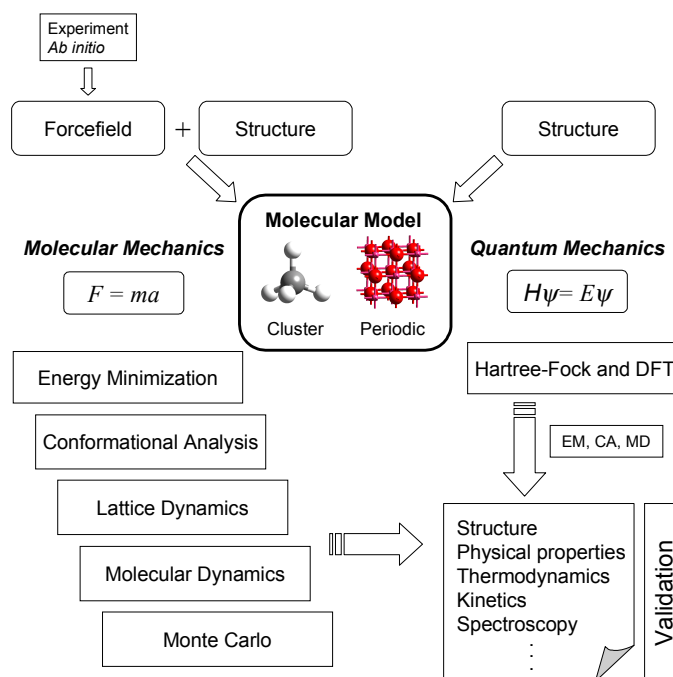


**Figure 2.** Flow diagram for molecular mechanics and quantum mechanics methods showing input requirements, various approaches, and output possibilities. Molecular model can be comprised of an isolated molecular cluster or a periodic cell.

used to examine the structure and energy of either a molecule or periodic system. The molecule can be treated as an isolated entity (gas phase molecule) or solvated (by using an advance modeling approach) ion or molecule. Periodic systems include crystalline structures, glasses, and other amorphous materials. Glasses and explicitly solvated molecules often rely on the use of large periodic simulation cells to realistically represent the long-range disorder of solution molecules or glass components while avoiding edge and surface effects.

Molecular mechanics methods rely on the use of analytical expressions that have been parameterized, through either experimental observation or quantum calculations, to evaluate the interaction energies for the given structure or configuration. Various modeling schemes are then used to evaluate the potential energy and forces on the atoms to obtain optimized or equilibrated configurations for the molecule or periodic system. Energy minimization, conformational analysis, molecular dynamics, and stochastic methods are important tools in molecular mechanics. Molecular dynamics simulations directly involve the calculation of forces based on Newtonian physics ( $F=ma$ ) and provide a deterministic basis for evaluating the time evolution of a system on the time scale of pico- and nanoseconds. In contrast, quantum mechanics uses first principles methods without the need of empirical parameters, for most instances, to evaluate the energy of the system. The Schrödinger wave equation—or more exactly, an approximation to the Schrödinger equation—is solved by a variety of methods to obtain the total energy of the molecule or periodic system. As with molecular mechanics, minimization and dynamics methods can be implemented, however, these advanced quantum techniques can lead to extreme computational costs especially for large-atom systems. Ultimately, either approach leads to the prediction of structure and physical properties, and the determination of thermodynamic, kinetic, and spectroscopic properties. A successful molecular simulation will provide validation with experiment and lead to further refinement of the model to support its relevance to the physical world.

This chapter provides an overview of the theory, methods, and philosophy of molecular modeling and simulation. Although meant to address specific applications associated with mineralogical and geochemical problems, numerous examples of simple molecular and crystalline models, some involving organic compounds, are presented. The level of the content is geared towards the novice and assumes no previous experience with molecular simulation. More detailed reviews are offered in the following chapters, or in the numerous references cited in this and other chapters of the book. Due to the scope and complexity of the subject matter, the reader will be subjected to presentations in this volume that involve various measurement units, especially those for energy. Rather than conform to one single unit system throughout the book, the chapters rely on the conventional units associated with the modeling method, and which have typically evolved with the literature for that particular discipline. It is obvious that chemists and physicists may never come to an agreement on the use of a consistent unit system. Table 1 provides a helpful set of conversion units to sort through these various unit schemes. Several values for the universal constants are also included. A glossary presented at the end of the chapter may also be useful in sorting through the terms and methods used throughout this volume.

An important reminder on the use of molecular modeling is provided by the second of the quotes presented at the beginning of this chapter. Manfred Eigen, a Noble-winning electrochemist, succinctly identified the number one failing common to those using molecular modeling methods. No matter how rigorous or uncompromising the theory is behind the model used to examine a chemical process, the model may completely miss the mark and be totally irrelevant. Tread carefully, and maintain a strong sense of validation with experimental and field observations!

**Table 1.** Physical constants and conversion factors

|                        |                  |   |
|------------------------|------------------|---|
| Avogadro constant      | $N_A$            | $6.022045 \times 10^{23}$ /mol                |
| Boltzmann constant     | $k$              | $1.38066 \times 10^{-23}$ J/K                 |
| Gas constant           | $R = kN_A$       | 8.31441 J/K mol                               |
| Elementary charge      | $e$              | $1.602177 \times 10^{-19}$ C                  |
| Faraday constant       | $F = eN_A$       | $9.6485 \times 10^4$ C/mol                    |
| Planck constant        | $h$              | $6.62618 \times 10^{-34}$ J s                 |
|                        | $\hbar = h/2\pi$ | $1.05459 \times 10^{-34}$ J s                 |
| Bohr radius            | $a_o$            | 0.5292 Å                                      |
| Mass of electron       | $m_e$            | $9.10939 \times 10^{-31}$ kg                  |
| Velocity of light      | $c$              | $2.99792458 \times 10^8$ m/s                  |
| Permittivity of vacuum | $\epsilon_o$     | $8.85419 \times 10^{-12}$ C <sup>2</sup> /J m |
| 1 kJ/mol               | =                | 0.2390 kcal/mol                               |
| 1 erg                  | =                | $1.4393 \times 10^{13}$ kcal/mol              |
| 1 eV                   | =                | 23.0609 kcal/mol                              |
| 1 rydberg              | =                | 318.751 kcal/mol                              |
| 1 hartree              | =                | 627.51 kcal/mol                               |
| 1 cm <sup>-1</sup>     | =                | $2.8591 \times 10^{-3}$ kcal/mol              |

## POTENTIAL ENERGY

The most important requirement of any molecular mechanics simulation is the forcefield used to describe the potential energy of the system. An accurate energy forcefield is the key element of any successful energy minimization, Monte Carlo approach, or molecular dynamics simulation. The forcefield includes interatomic potentials that collectively describe the energy of interaction for an assemblage of atoms in either a molecular or crystalline configuration. Analytical expressions of the forcefield are typically obtained through the parameterization of experimental and spectroscopic data, or in some cases, by the use quantum mechanical calculations. The potential energy can then be presented as a function of distance, angle, or other geometry measurement. The analytical functions typically are quite simple and describe two- three- or four-body interactions. It is then possible to describe the potential energy of a complex multi-body systems by the summation of all energy interactions over all atoms of the system. In principle, an accurate description of the potential energy surface of a system can be obtained by the forcefield as a function of the geometric variables.

### Energy terms

The total potential energy of a system can be represented by the addition of the following energy components:

$$E_{Total} = E_{Coul} + E_{VDW} + E_{Bond\ Stretch} + E_{Angle\ Bend} + E_{Torsion} \quad (1)$$

where  $E_{Coul}$ , the Coulombic energy, and  $E_{VDW}$ , the van der Waals energy, represent the so-called nonbonded energy components, and the final three terms represent the explicit bonded energy components associated with bond stretching, angle bending, and torsion

dihedral, respectively. The Coulombic energy, or electrostatics energy, is based on the classical description of charged particle interactions and varies inversely with the distance  $r_{ij}$ :

$$E_{Coul} = \frac{e^2}{4\pi\epsilon_0} \sum_{i \neq j} \frac{q_i q_j}{r_{ij}} \quad (2)$$

Here,  $q_i$  and  $q_j$  represents the charge of the two interacting atoms (ions),  $e$  is the electron charge, and  $\epsilon_0$  is the permittivity (dielectric constant) of a vacuum. The summation represents the need to examine all possible atom-atom interactions while avoiding duplication. Equation (2) will yield a negative and attractive energy when the atomic charges are of opposite sign, and a positive energy, for repulsive behavior, when the charges are of like sign. In the simple case, the Coulombic energy treats the atoms as single point charges, which in practice is equivalent to spherically-symmetric rigid bodies.

Simulations involving crystalline materials or other periodic systems require the use of special mathematical methods to ensure proper convergence of the long-range nature of Equation (2); the  $1/r$  term is nonconvergent except for the most simple and highly symmetric crystalline systems. In practice, it is therefore necessary to employ the Ewald method (Ewald 1921) or other alternative method (e.g., Greengard and Rokhlin 1987; Caillol and Levesque 1991) to obtain proper convergence and an accurate calculation of the Coulombic energy. The Ewald approach replaces the inverse distance by its Laplace transform that is decomposed into two rapidly convergent series, one in real space and one in reciprocal space (Tosi 1964; de Leeuw et al. 1980; Gale, this volume). The Coulombic energy in ionic solids typically dominates the total potential energy and, therefore, controls the structure and properties of the material. Purely ionic compounds such as the metal halide salts (e.g., NaF and KCl) are examples where the formal charge is used to accurately represent the electrostatics. In molecular systems where covalent bonding is more common, the Coulombic energy is effectively reduced by the use of partial or effective charges for the atoms. The Coulombic energy for non-periodic systems can be evaluated by direct summation without resorting to Ewald or related periodic methods.

The van der Waals energy represents the short-range energy component associated with atomic interactions. Electronic overlap as two atoms approach each other leads to repulsion (positive energy) and is often expressed as a  $1/r^{12}$  function. An attractive force (negative energy) occurs with the fluctuations in electron density on adjacent atoms. This second contribution is referred to as the London dispersion interaction and is proportional to  $1/r^6$ . The most common function for the combined interactions is provided by the Lennard-Jones expression:

$$E_{VDW} = \sum_{i \neq j} D_o \left[ \left( \frac{R_o}{r_{ij}} \right)^{12} - 2 \left( \frac{R_o}{r_{ij}} \right)^6 \right] \quad (3)$$

where  $D_o$  and  $R_o$  represent empirical parameters. Although various forms of the 12-6 potential are used in the literature, the form presented above provides a convenient expression that equates  $D_o$  to the depth of the potential energy well and  $R_o$  to the equilibrium atomic separation. This association would only apply for the interaction of uncharged atoms (e.g., inert gases), however, the functionality is used in practice for partial and full charge systems. Alternatively, a 9-6 function or a combined exponential- $1/r^6$  (Buckingham potential with three fitting parameters), among other functions, can be

used to express the short-range interactions. In contrast to the long-range nature of the Coulombic energy, the van der Waals energy is non-negligible at only short distances (typically less than 5 to 10 Å), and, therefore in practice, a cutoff distance is used to reduce the computational effort in the evaluation of this energy.

Some energy forcefields are based on the simple ionic Born model such that only the first two terms of Equation (1) are used. If properly parameterized, the inclusion of just the Coulombic and van der Waals (short-range) terms for the total potential energy is more than satisfactory for successfully modeling the structure and physical properties of numerous oxides and silicates phases (e.g., Lewis and Catlow 1986). Often the shell model of Dick and Overhauser (1958) is used as a refinement of the ionic model by incorporating electronic polarization of the ions. The shell model uses two point charges joined by a harmonic spring (based on a  $1/2 kx^2$  potential) to represent the polarization of an ion; the negatively-charged electron shell is associated with a positive nucleus-like core. The modification provides a necessary extension of the ionic model for modeling point defects in solids and surface structures where large asymmetric electrostatic potential fields will induce significant polarization among the ions, especially polarizable anions like oxygen. Elastic, dielectric, diffusion, and other materials properties can be accurately derived using the refinement provided by the shell model. Alternative polarization models (e.g., Agnon and Bukowinski 1990; Zhang and Bukowinski 1991) have also proven to be reliable in simulating oxide systems.

The shell model is an attempt to treat a form of covalency in an ionic solid. However, the total-energy treatment of bonded systems requires the addition of several so-called bonded terms. The first of the bonded terms of Equation (2), the bond stretch term can be represented as a simple quadratic (harmonic) expression:

$$E_{Bond\ Stretch} = k_1(r - r_o)^2 \quad (4)$$

where  $r$  is the separation distance for the bonded atoms,  $r_o$  is the equilibrium bond distance, and  $k_1$  is an empirical force constant. This relation ensures that the two atoms will interact through a potential that allows vibration about an equilibrium bond distance. In fact, the force constant  $k_1$  can be obtained directly from analysis of the vibrational spectrum. Alternatively, a Morse potential can be used to provide a more realistic description of the energy of a covalent bond:

$$E_{Morse} = D_o [1 - \exp\{1 - \alpha(r - r_o)\}]^2 \quad (5)$$

Here,  $D_o$  represents the equilibrium dissociation energy and  $\alpha$  is a parameter related to the vibrational force constant. Figure 3 provides a comparison of the two potential functions used to describe the carbon-hydrogen bond stretch based on the Dauber-Osguthorpe et al. (1988) forcefield parameters. Although both represent the equilibrium bond distance of 1.105 Å, the anharmonic nature of the Morse potential provides a more satisfying description of the C-H dissociation that would be expected at large bond distances. The harmonic potential is only suitable at near-equilibrium configurations where only small distortions of the bond occur. Nonetheless, unless a structure is perturbed to extreme C-H distances (beyond 0.2 Å), the harmonic potential represents the potential energy for the bond quite well. Non-bonded interactions, as discussed above, are usually ignored once a bond has been defined between two atoms.

A harmonic potential is typically used to describe the angle bend component for a bonded system. Equation (6) provides this energy expression in terms of an angle bend force constant  $k_2$  and the equilibrium bond angle  $\theta_o$ :

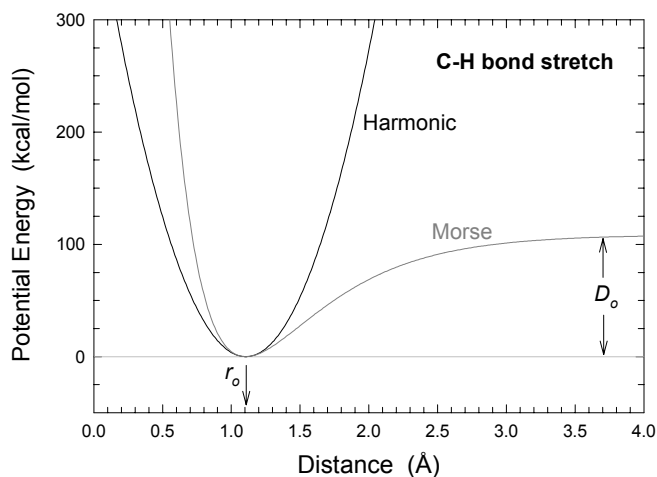


**Figure 3.** Comparison of harmonic and Morse potentials to represent the bond stretch energy of the carbon-hydrogen bond. The Morse potential is more appropriate for modeling significant deviations from the equilibrium atom separation distance  $r_0$ ;  $D_0$  is the bond dissociation energy.

$$E_{\text{Angle Bend}} = k_2(\theta - \theta_0)^2 \quad (6)$$

This expression necessarily requires a triad of sequentially bonded atoms, such as H-O-H in water or H-C-H in methane, where  $\theta$  is the measured bond angle for the configuration. As with the harmonic potential for bond stretch, deviations from an equilibrium value will increase the energy and destabilize the configuration. The final bonded term of Equation (1) is that for the four-body torsion dihedral interactions. The dihedral angle  $\phi$  is defined as the angle formed by the terminal bonds of a quartet of sequentially bonded atoms as viewed along the axis of the intermediate bond. An example of the analytical expression for the torsion energy is provided by:

$$E_{\text{Torsion}} = k_3(1 + \cos 3\phi) \quad (7)$$

where  $k_3$  is an empirical force constant. The use of the trigonometric function ensures that a periodicity is followed for the dihedral angle variation, which is related to the atomic orbital hybridization of the intermediate atoms (e.g.,  $120^\circ$  period for  $sp^3$  hybridization). The geometry measurements for the bond angle and torsion terms are represented in Figure 4 for the case of methane and dichloroethane.

Additional terms can be added to the total potential energy expression of Equation (2), such as an out-of-plane stretch term for systems that have a planar equilibrium structure (e.g.,  $\text{CO}_3^{2-}$  groups). More sophisticated energy forcefields, usually involving

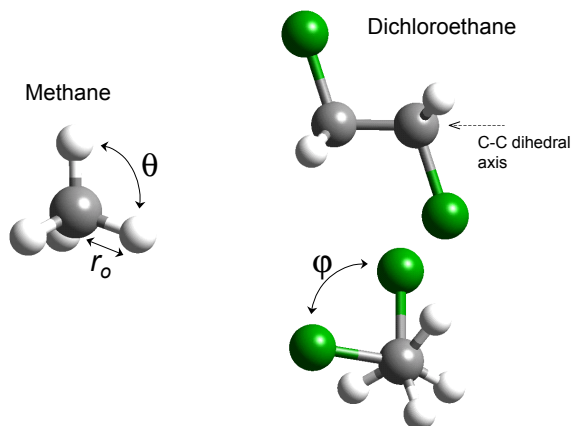


**Figure 4.** Geometry parameters for bond stretch and angle bend as noted on the energy-minimized structure of methane (left), and for bond torsion for dichloroethane (right). The axis used for defining the torsion angle is indicated along C-C bond in the energy-minimized structure of dichloroethane (upper right) with  $\phi = 180^\circ$  for the Cl-C-C-Cl torsion. A less stable configuration based on a smaller dihedral angle is presented in a conformer structure viewed looking down the C-C bond (bottom right).

well-characterized organic systems, often incorporate cross terms among each of the bonded energy terms in order to accurately model the experimental vibrational frequencies of molecules. Unfortunately, details on these complex modes of interaction for most geological materials are unknown—their contributions are quite small—and therefore the cross terms are ignored in the parameterization. Finally, external perturbations to the molecular system can be included in the total potential energy expression. These include energy terms for the addition of a hydrostatic pressure or for directional stresses and electric fields.

### **Atomic charges**

Atomic charges are an integral part of any energy forcefield and are not to be assigned arbitrarily. The non-bonded Buckingham potential typically incorporates a full ionic charge to represent the charge on the atom. The inclusion of a shell model in the Buckingham potential requires that the ionic charge be proportioned between the core and shell components to collectively produce the full ionic charge. Molecular models relying on a bonded potential will always be represented by reduced partial charges. A bonded potential assumes that the Coulombic energy associated with an atom is reduced by the transfer of the valence electrons to the bond. The bond stretch energy is introduced to represent this contribution, thereby requiring that the charges on the atoms be reduced. There are various schemes available to assign these partial charges, one of which is the charge equilibration scheme of Rappé and Goddard (1991) based on the geometry, ionization potentials, electron affinities, and radii of the component atoms. There are other simpler empirical schemes that use the coordination, connectivity, and bond order to assign partial charges. Experimental approaches, usually based on deformation electron densities derived from high-resolution X-ray diffraction analysis, often provide accurate charge values (Coppens 1992; Spasojevicde-Bire and Kiat 1997). However, the most helpful and convenient approach for charge assignment relies on high-level quantum mechanical calculations. Typically, these calculations are performed on clusters or simple periodic systems that best represent the chemical environment. The electrostatic potential (ESP), derived from the electron densities, are then used in a least-squares fit to obtain the optimum atomic charges that reproduce the electrostatic potential. Programs such as CHELPG (Chirlian and Francl 1987; Breneman and Wiberg 1990) are helpful in obtaining these ESP-based atomic charges. Similarly, Mulliken electron analysis (Mulliken 1955) can be used to derive atomic charges based on the populations of the molecular orbitals and contributing atomic orbitals, however, this method is less sophisticated and often leads to ambiguous charge assignments.

### **Practical concerns**

The exact nature of the analytical functions used to express any of the potential energy components is not the critical point of this discussion. It is important that the parameterization be as accurate as possible toward reproducing the observed data (experimental or quantum-based) to ensure that the molecular simulation reproduces the correct energies (and approximate shape of the energy surface) for the molecular model. A greater number of parameters for an energy function may ensure a more accurate representation, however, the computational cost may become prohibitive as the more complex functions are evaluated at each stage of a simulation, often over a million times. Methods to reduce the computational effort, especially for large molecular systems and simulation cells, are required. Additionally, symmetry, cell constraints, or fixed atomic positions can be incorporated in the molecular mechanics simulation.

In theory, quantum chemical methods could be used to calculate the potential energy surface of a system and therefore forego with the parameterization of a forcefield.

Essentially, the Schrödinger equation is solved to obtain a set of molecular orbitals that represent the lowest energy state for the molecule or periodic system. However, in practical terms, the computational cost becomes prohibitive, especially for large systems (typically greater than 20 atoms), as numerous geometries and configurations require calculation of their electronic structure and potential energy. Even for the case of approximate or semi-empirical quantum methods, or those using a limited atomic basis set, energy calculations would be impractical for most molecular modeling needs. Nonetheless, some progress has been made in this research area, specifically in quantum dynamics simulations using massively-parallel computers (see below).

## MOLECULAR MODELING TECHNIQUES

### Conformational analysis

One of the more valuable uses of molecular mechanics is the ability to test the energetics and relative stabilities of various molecular configurations. Conformational analysis provides a means of monitoring the relative stabilities of various conformers for a molecular system. Conformers, or conformational isomers, represent the various arrangements of atoms that can be converted into one another by rotation about a single bond. Figure 5 provides an example of the relative stabilities of various conformations of the carcinogen dichloroethane based on the torsional rotation about the carbon-carbon bond. The 1,2-dichloroethane isomer, also known as dichloroethylene, has several stable configurations represented by the three minima in the total energy plot (lower part of Fig. 5). The lowest energy conformer is the *anti* configuration where the chlorine atoms are furthest apart. The other two minima are associated with conformers in the stable *gauche*

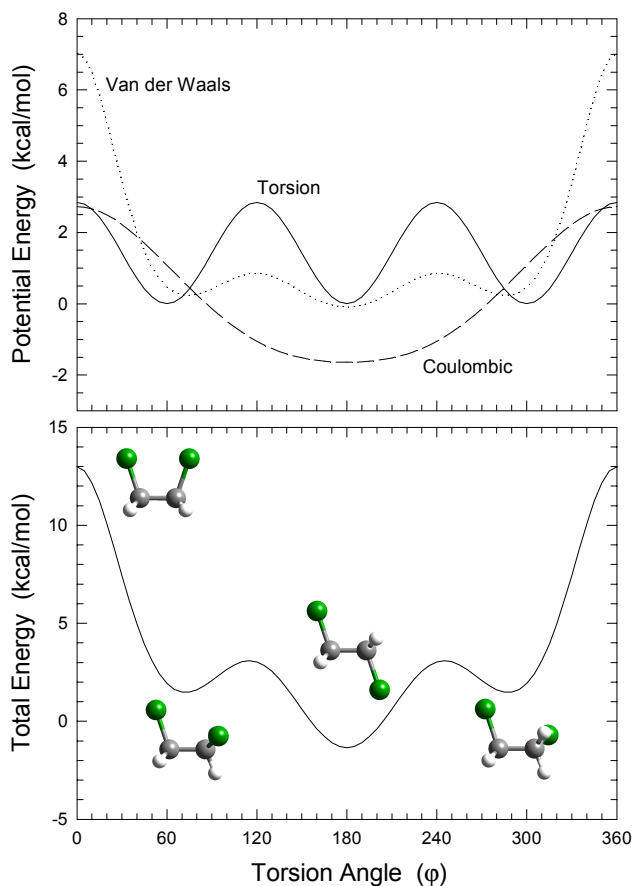


**Figure 5.** Component (upper) and total (lower) potential energy for dichloroethane as a function of the torsion angle defined by Cl-C-C-Cl. Structural models corresponding to the three stable conformers (two local minima and one global minimum) and the least stable transition structure are provided in the total energy plot.

configuration where the one chlorine atom is staggered between the other chlorine and a hydrogen. The least stable conformer is the transition configuration having the chlorine atoms fully eclipsed.

The upper part of Figure 5 presents the components of the total potential energy as a function of the torsion angle. The component energies were obtained using the forcefield parameters of Dauber-Osguthorpe et al. (1988) in which seven bonds, twelve angles, and nine torsion terms, in addition to the nonbonded Coulombic and van der Waals energies, were evaluated for each molecular configuration. Bond distances and bond angles were kept fixed while evaluating the energy changes associated with the carbon-carbon torsion. The coincidence of the component energy minima, especially with the strong influence of the Coulombic energy, helps to stabilize the *anti* configuration. The short-range repulsive component of the van der Waals energy controls the destabilization of the eclipsed configuration. The relatively small energy barriers associated with the *gauche* to *anti* transitions (approximately 2 kcal/mol) suggest that at room temperature all three of the most stable conformers would exist. This assumes the forcefield is accurately representing the enthalpy of these interactions. The *anti* to *gauche* transition has an energy barrier of 4.5 kcal/mol and would also occur at room temperature. In contrast, the large energy barrier associated with the eclipsed conformation is substantial and one would expect significant inhibition toward this transition.

Although, at first, this example might be considered chemically intuitive, the use of molecular mechanics provides a strong theoretical basis to evaluate and identify the contributing components that control the stabilization of the molecule. Furthermore, larger and more complex molecules and periodic systems that have significantly greater configuration possibilities are only amenable to conformational analysis through computational methods. Sampling of optimal configurational space for large systems becomes more of a fine art than a simple matter of brute force energy calculations. Techniques such as Monte Carlo analysis and thermal annealing assist in this sampling effort, and are discussed later in the chapter.

### Energy minimization

Energy minimization, also referred to as geometry optimization, is a convenient method in molecular mechanics (and quantum mechanics) for obtaining a stable configuration for a molecule or periodic system. The procedure involves the repeated sampling of the potential energy surface until the potential energy minimum is obtained corresponding to a configuration where the forces on all atoms are zero. The energy of an initial configuration is first determined then the atoms (and cell parameters for a periodic system) are adjusted using the potential energy derivatives to obtain a lower energy configuration. This procedure is repeated until defined tolerances for the energy difference and derivatives between successive steps are achieved. Careful attention is needed for complex systems where structures associated with local energy minima may be obtained rather than the most stable configuration at the true global energy minimum. Multiple initial configurations or more advanced modeling techniques are required to ensure the attainment of the global energy minimum structure. Several algorithms are typically used in energy minimization procedures. Line searches and steepest gradient methods, and the more complex conjugate gradient and Newton-Raphson methods are often used in this effort. They can be used independently or collectively to obtain the lowest energy configuration. The Newton-Raphson approach evaluates both first and second derivatives of the energy to identify an efficient search path for locating the energy minimum configuration. Leach (1996) provides an excellent description of the various energy minimization techniques.

Special conditions or constraints on the chemical system can be imposed during the energy optimization or other molecular simulation. Molecular and crystallographic symmetry can be constrained during the optimization or the atomic positions can be fixed. Periodic systems can have all cell parameters vary to simulate constant pressure conditions so that no net force occurs on the simulation cell boundaries. Fixing the cell parameters corresponds to a constant volume optimization, but this may result in the significant buildup of forces on the cell faces, especially if the cell parameters are far from their equilibrium values. A successful energy optimization is often performed without constraints of any kind. For a periodic system, this corresponds to a simulation cell having P1 symmetry where there is no symmetry imposed on the atomic positions (other than translational symmetry) and all six cell parameters are allowed to vary.

Lattice dynamics simulations provide a powerful extension of energy minimization methods by evaluating the dynamical matrix that relates forces and atomic displacements for a crystal. Originally developed by Born and Huang (1954), this method incorporates a statistical mechanics approach to determine the vibrational modes and thermodynamic properties of a material. Examples of lattice dynamics calculations are noted in a later section of this chapter, and Parker et al. (this volume) presents a detail discussion of the technique for use in examining various minerals and mineral surfaces.

### Energy minimization and classical-based equilibrium structures

An example of how two charged atoms interact to form an equilibrium configuration is provided in Figure 6 for the case of an isolated magnesium and oxygen. A Buckingham potential is used to describe the interatomic potential based on the rigid ion parameters of Lewis and Catlow (1986) and Jackson and Catlow (1988) and which use full formal charges for the atoms. The total potential energy expression is given by:

$$E_{MgO} = k \frac{q_{Mg} q_O}{r_{MgO}} + A \exp(-r_{MgO} / \rho) - \frac{C}{r_{MgO}^6} \quad (8)$$

where  $k$  is a unit conversion factor,  $A$ ,  $\rho$ , and  $C$  are empirical parameters. The short-range contribution to the potential energy is positive and rapidly increases at short distances. The Coulombic energy associated with the oppositely charged ions is negative and leads to stabilization as the two ions approach each other. The summation of the two terms provides the total energy characterized by an energy minimum that corresponds to the equilibrium separation distance for the atoms. Alternatively, partial charges less than the formal charge can be used to describe the same Mg-O interaction. Figure 7 presents a

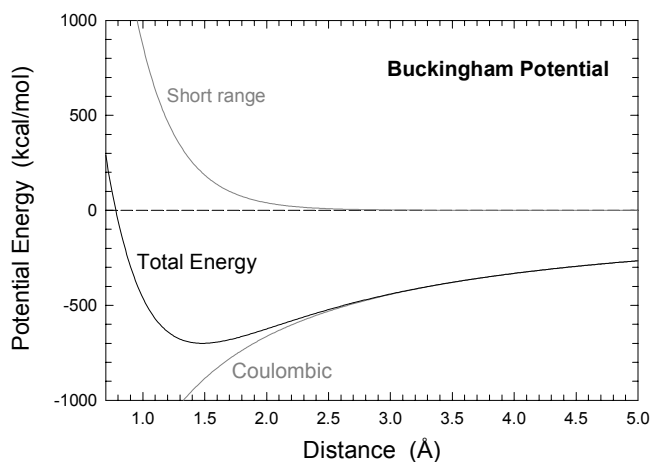


**Figure 6.** Potential energy as a function of separation described by a Buckingham potential for Mg-O ionic interactions. The total energy curve is characterized by a minimum corresponding to the equilibrium separation distance.

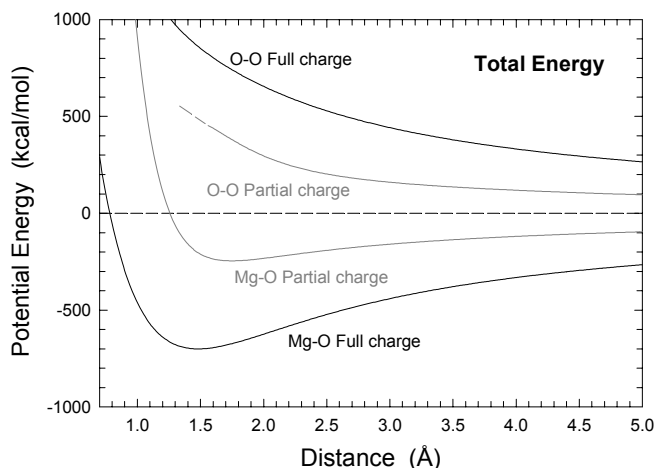


**Figure 7.** Comparison of partial charge and full ionic charge Buckingham models for the potential energy of Mg-O interactions as a function of separation distance.

comparison of the full charge Mg-O and O-O Buckingham potentials (Lewis and Catlow 1986; Jackson and Catlow 1988) with those derived from quantum methods and using partial charges (Teter 2000). The latter potential uses reduced charges of  $q_{Mg} = 1.2$  and  $q_O = -1.2$ . Both sets of O-O potentials are included to show the destabilization of similarly-charged ions with decreasing distance, where the total energy does not exhibit an energy minimum. In contrast, the Mg-O total energy curves exhibit minima denoting equilibrium distances of 1.48 Å and 1.75 Å, respectively, for the full charge and partial charge potential models. Note that these distances are significantly shorter than the Mg-O bond distance (2.10 Å) in crystalline periclase (MgO). The full charge potentials for Mg-O and O-O are characterized by larger contributions of the Coulombic energy leading to greater destabilization for the O-O interaction and a deeper potential well for the Mg-O interaction. Yet, given these differences in interatomic potentials, both sets of forcefield potentials provide excellent results for the simulating the crystalline structure of periclase.

The results for periclase simulations are presented in Figure 8 where the total potential energy is plotted as a function of periclase cell parameter. Periclase has the rock salt structure and is characterized by perfect regular octahedral coordination. Because of the high symmetry limiting structural variation to only the cell parameter, calculation of the total potential energy—which for crystalline materials is known as the lattice

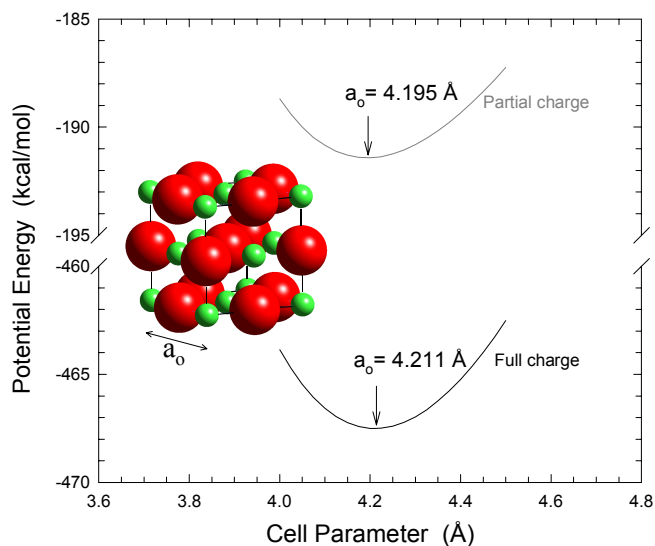


**Figure 8.** Comparisons of potential energy for the crystal structure of MgO as a function of cell parameter  $a_o$  based on partial charge and full charge Buckingham potentials.

energy—is a straightforward matter. Both sets of forcefield parameters provide similar energy-minimized structures with nearly identical cell parameters that are in excellent agreement with the observed value of 4.211 Å (Hazen 1976). Also, both potential sets provide similar shapes for the energy-distance curves, of which the curvature represents the vibrational characteristics of the material. Two additional sets of potentials that incorporate a shell model to describe the oxygen polarization provided comparable results. The significant displacement of the full charge potential to lower energy is related to the greater significance of the Coulombic term in the full charge potential. In contrast to molecular systems where bonded forcefields are typically used, it is difficult to relate the forcefield parameters used in non-bonded potentials to the results of calculations where the long-range Coulombic forces are strong and occur across all anion-anion and cation-cation interactions, and not just cation-anion pairs. This is the reason for the large differences in distance values at the energy minima for the two-atom examples in Figure 7 and those for the full crystal periodic simulations of Figure 8.

### Quantum chemistry methods

The application of quantum mechanics to topics of mineralogical and geochemical interest is perhaps the most intriguing and challenging task for computational chemists. In implementing these electronic structure calculations, the modeler is no longer restricted to the classical description of using the balls and springs of molecular mechanics methods to describe the complex interactions of atoms and molecules. Now, by solving the Schrödinger equation for larger and more complex systems, albeit through approximate methods, the quantum chemist can obtain energies, molecular and crystalline structures and properties, electrostatic potentials, an analysis of spectroscopic data, thermodynamic properties, a detailed description of reaction mechanisms, and non-equilibrium structures. A quantum chemistry approach brings the electrons to the forefront of the molecular model by allowing the modeler to probe the distribution of electrons among the mathematical wavefunctions that describe the molecular orbitals for the system.

The time-independent Schrödinger equation is given by the following eigenfunction relation:

$$H\Psi = E\Psi \quad (9)$$

where  $H$  is the Hamiltonian differential operator,  $\Psi$  is the wavefunction, and  $E$  is the total energy of the system. The Hamiltonian is comprised of kinetic and potential energy components just as in a classical mechanics. Equation (9) can therefore be restated as:

$$\left( -\frac{h^2}{8\pi^2} \sum_i \frac{1}{m_i} \nabla^2 + \sum_{i \neq j} \frac{e_i e_j}{r_{ij}} \right) \Psi = E\Psi \quad (10)$$

where  $h$  is Planck's constant,  $m$  is the mass,  $\nabla^2$  is the Laplacian operator, and  $e$  is the charge of the particles (either electrons or nuclei) at separation distance  $r_{ij}$ . The second term of this expression represents the potential energy associated with the Coulombic interactions of all nuclei and electrons of the system. There are several restrictions on the nature of the wavefunction in order to satisfy the Schrödinger equation for electronic structure calculations (e.g., symmetry, Pauli exclusion, and choice of eigenstates). Additionally, the wavefunction provides the critical role in determining the probability distribution function for electrons in configurational space (i.e., orbital geometry), and for obtaining the energy of the system as the expectation value of the Hamiltonian. Unfortunately, Equation (10) has an exact analytical solution for only the one electron system, and therefore approximations must be made to apply quantum mechanics to the

many-electron systems of molecules and materials of interest. The Born-Oppenheimer approximation that effectively decouples nuclear and electronic motions, and the combining of one-electron orbitals to describe the total wavefunction contribute to this effort.

Excellent discussions of the various quantum methods that are commonly used today to solve the Schrödinger equation are provided in several review articles and textbooks. Among those that are noteworthy, especially with regard to their readability and application to inorganic and crystalline materials, are Hehre et al. (1986), Labanowski and Andzelm (1991), Springborg (1997), and especially the recent book of Cook (1998). The comprehensive volume by Tossell and Vaughan (1992) is very helpful in providing numerous geochemical examples involving quantum methods. Of course, several of the following chapters in this book provide a state-of-the-art perspective on quantum methods and applications to the geosciences. Also of special note are the reviews of Gillan et al. (1998) and Billing (2000) in which they discuss the role of quantum chemistry in modeling surfaces and molecule-surface interactions. Lasaga (1992) presents a similar review but with particular application to mineral surface reactions.

Quantum chemistry methods can be divided into four distinct classes: *ab initio* Hartree-Fock methods, *ab initio* correlated methods, density functional methods, and semi-empirical methods (Hehre 1995). *Ab initio* refers to “from the beginning”, and consequently these first principles methods do not use any empirically or experimentally-derived quantities. Hartree-Fock methods use an antisymmetric determinant of one-electron orbitals to define the total wavefunction. Electrons are treated individually assuming the distribution of other electrons is frozen and treating their average distribution as part of the potential. The wavefunction orbitals and their coefficients are refined through an iterative process until the system reaches a steady result, or self-consistent field. Correlated methods extend the Hartree-Fock approach by introducing a term in the Hamiltonian that corrects for local distortion of an orbital in the vicinity of another electron. The Hartree-Fock approach assumes the entire orbital is affected in an averaged sense. Standard Hartree-Fock methods still perform quite favorably in predicting equilibrium geometries compared to correlated or density functional methods, however the lack of electron correlation typically leads to inaccurate force constants and vibrational frequencies. Perturbation calculations associated with the correlated methods can often become quite costly for the sake of improving calculations to this level of accuracy. Gibbs (1982), and Lasaga (1992) provide insightful reviews of applications of *ab initio* methods to mineralogy and geochemistry.

The third class of quantum methods includes those based on density functional theory (DFT) that incorporate exchange and correlation functionals of the electron density based on a homogeneous electron gas, and evaluated for the local density of the system. The density of the electrons rather than the wavefunction is used in DFT to describe the energy of the system. The theory was developed in the early 1960's (Hohenberg and Kohn 1964; Kohn and Sham 1965), and led to the awarding of 1998 Nobel Prize in chemistry to the Walter Kohn. A general review of DFT methods and applications is provided by Jones and Gunnarsson (1989). The local density approximation (LDA) provides quite accurate results for a wide range of molecules and crystalline systems (Kohn and Sham 1965). A more sophisticated refinement of DFT is the generalized gradient approximation (GGA) in which the gradient of the charge density is utilized (Perdew et al. 1996). DFT methods have become the method of choice in recent years among computational chemists primarily due to the economy in efficiently scaling with the number of electrons in the system—at  $N^3$  compared to  $N^4$  or greater for standard Hartree-Fock methods. Plane-wave pseudopotential methods, originally developed by the

solid-state physics community, provide a computationally efficient DFT approach for periodic systems in which only the valence electrons of the atoms are explicitly treated, and represented by a plane-wave expansion. Teter et al. (1989), Payne et al. (1992), and Milman et al. (2000) provide excellent reviews of the theory and applications of plane-wave pseudopotential and DFT methods to large-atom periodic systems. Additionally, a hybrid quantum approach that combines the electron densities derived from standard Hartree-Fock theory with the DFT functionals has also been widely used (Gill et al. 1992; Oliphant and Bartlett 1994).

The semi-empirical methods involve some empirical input into obtaining approximate solutions of the Schrödinger equation. Typically, this class of approximate methods avoids the computational cost of evaluating the numerous electron repulsion integrals that make *ab initio* methods so computationally expensive. A general description of the various semi-empirical methods is provided by Pople and Beveridge (1970). Because of the success of DFT methods and access to faster and more powerful computers, in addition to the inaccuracies and limitations of the approach, semi-empirical methods are no longer as common in the chemistry literature as they were twenty years ago.

### Energy minimization and quantum-based equilibrium structures

As with classical molecular mechanics, quantum methods provide a means for obtaining equilibrium configurations based on an analysis of the total energy using a minimization procedure. Figure 9 presents the energy-minimized structure obtained from the gas phase analysis of methane (isolated molecule), for comparison with that derived from classical methods (cf. Fig. 4). A DFT approach involving GGA functionals and a double numeric basis set including polarization functions was used to calculate the equilibrium structure (Delley 1990). Geometry optimization was based on an efficient gradient scheme that involves the internal coordinates of the molecule (Baker 1993). The

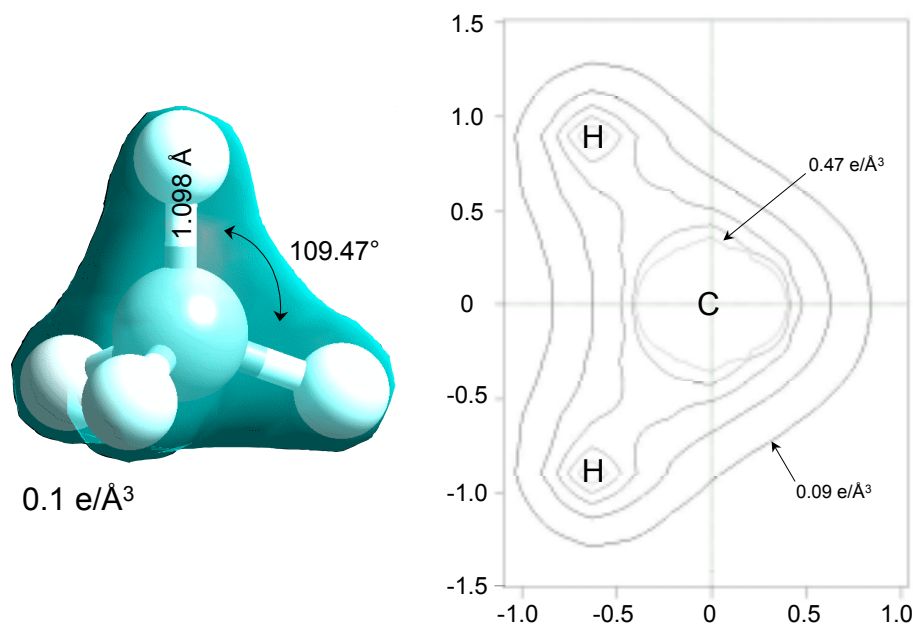


**Figure 9.** Energy-optimized structure of methane (left) derived from a high-level DFT calculation and showing the extent of the  $0.1 \text{ e}/\text{\AA}^3$  electron density contour superimposed onto the ball-and-stick representation of the molecule. A slice of the electron density taken through one of the C-H-H planes (right) shows the covalent nature of the C-H bond with the buildup of charge along the C-H axes.

calculated C-H bond distances and H-C-H bond angles are in excellent agreement with experimental values. As expected, the C-H bond distance is similar to the equilibrium value associated with the Morse potential as described earlier for use in a classical forcefield. Analysis of the final wavefunctions for the optimized methane structure provides the electron density, or charge density, for determining the distribution of the ten electrons in the molecule. The extent of the  $0.1 \text{ e}/\text{\AA}^3$  isosurface is superimposed on the usual ball-and-stick model of methane in Figure 9. Also shown in Figure 9 is a slice of the electron density taken through one of the H-C-H planes. Both diagrams indicate the diffuse and asymmetric distribution of electrons in the molecule with electron buildup along each of the C-H bond axes, representing the strongly covalent bonds of methane, and at the atomic nuclei, representing the less significant role of the inner electrons in the molecular bonding.

Evaluation of the wavefunctions and electron densities provide theoretical dipole moments, optical polarizabilities, electrostatic potentials, atomic charges, and spatial distributions of the molecular orbitals. Frontier orbital theory based on the analysis of the highest occupied molecular orbital (HOMO) and lowest unoccupied molecular orbital (LUMO) provides insights into molecular reactivity as these are the orbitals most commonly involved in chemical reactions (Hehre 1995). Further analysis of molecular bonding using the Laplacian of the electron density to determine bond critical point properties and valence shell electron pair repulsions has been useful in evaluating the structure and reactivity of molecules and crystalline materials (Bader 1990; Gibbs et al., this volume). More sophisticated electronic structure calculations requiring gradient calculations (energy with respect to atomic displacement) for an energy-minimized structure are useful in obtaining vibrational frequencies (Kubicki, this volume) and NMR chemical shifts (Tossell, this volume). Additionally, transition states for reactive molecular configurations can be determined by identifying transition state maxima in the potential energy surface associated with the nearby stable minima (see Felipe et al., this volume).

The results of a plane-wave pseudopotential DFT calculation for periclase are presented in Figure 10. The periodic structure was optimized using the GGA method with ultrasoft potentials and a kinetic energy cutoff of 380 eV for the plane-wave expansion (Payne et al. 1992; Teter et al. 1995). Energy minimization was performed using the BFGS scheme described by Fischer and Almlöf (1992). The optimized structure for MgO

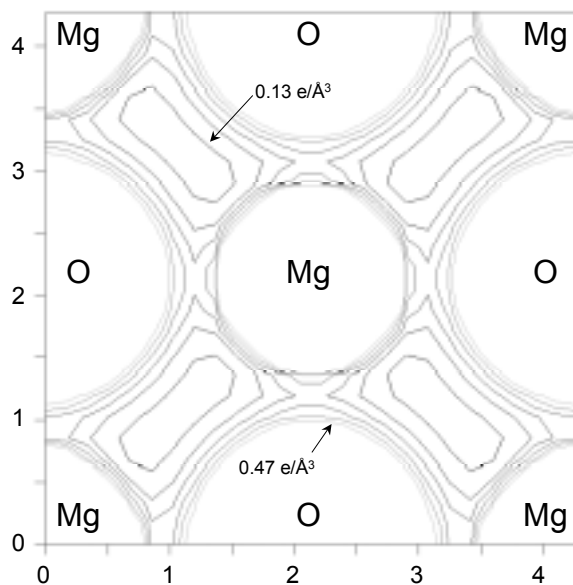


**Figure 10.** Slice of the electron density of MgO obtained from an optimization of the periodic structure using a nonlocal DFT approach with plane-wave pseudopotentials. The development of charge density and associated critical points between Mg and O atoms indicates the existence of covalent character in this material.

has a cell parameter of 4.270 Å that is slightly larger than the observed value of 4.211 Å (Hazen 1976) but is still respectable for the plane-wave pseudopotential technique. Part of this discrepancy is related to the use of the pseudopotential to describe the core electrons. Although the calculation is computationally faster than all-electron methods, there is a slight loss of accuracy in obtaining correct geometries. A slice of the electron density that passes through the atomic centers (Fig. 10) indicates that the charge is, as expected, lowest between Mg-Mg and O-O pairs. Most noteworthy in the electron density is the slight buildup of charge between neighboring Mg-O pairs suggesting the existence of some covalent bonding due to the overlap of orbitals. A Mulliken population analysis of the electron density and orbitals suggests approximately 30% covalent character for this material, although this may be high compared to experimental evidence (Souza et al. 1994). A purely ionic compound would exhibit spherically-symmetric charge density contours about the nuclei without any directional structure of the contours between atoms.

As with molecular systems, similar analysis of the wavefunctions and electron densities for periodic systems can help in evaluating various physical properties of the solid. These include electrostatic potential, spatial distribution of molecular orbitals including HOMO and LUMO, transition states, and vibrational frequencies. Additionally, equations of state and bulk moduli for the material can be derived from energy-volume curves (Cohen 1991; Stixrude et al. 1998; Stixrude, this volume). Geometry optimizations can be performed with fixed cell parameters (constant volume conditions), or the six lattice parameters can be allowed to vary (constant pressure conditions). Crystallographic symmetry can be imposed to constrain the atomic positions to symmetry sites during the energy minimization. Because of the high computational costs of obtaining fully optimized periodic structures with quantum chemistry codes, the use of space group symmetry and other constraints is extremely important.

### Monte Carlo methods

The stochastic analysis of the energetics of a chemical system is best represented by a Monte Carlo scheme in which a random sampling of the potential energy surface is performed in order to obtain a selection of possible equilibrium configurations. Monte Carlo-based molecular simulations predate molecular dynamics methods having been first introduced by Metropolis et al. (1953) for deriving the equation of state for a system comprised of two-dimensional rigid spheres. This approach obviates the need to calculate an entire regular array of configurations within a canonical ensemble; only a random sampling is required. The basics of the so-called Metropolis Monte Carlo method is described by the flow diagram presented in Figure 11. After an initial configuration for a system is defined and the total potential energy is determined, the model is randomly displaced (positioned) to a new configuration and a new energy is calculated. If the new configuration is more stable than the original, then the configuration is accepted and the spatial displacement operation is continued again.

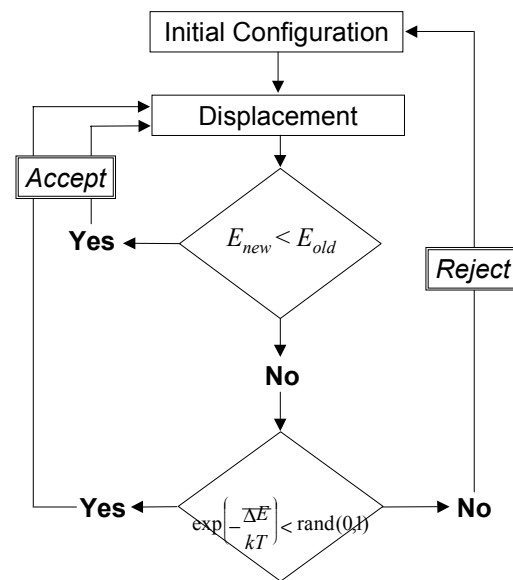


**Figure 11.** Flow diagram for the generalized Monte Carlo method in which a very large number of molecular configurations are compared to derive an optimal set of energetically-favored configurations.

However, if the new configuration energy is greater (less stable) than that for the original configuration, then the energy difference as part of a Boltzmann distribution is compared to a random number. If the value is less than the random number, then the configuration is accepted and used as the basis for a new displacement. If, however, the value is greater than the random number, then the new configuration is rejected and the previous configuration is used for the next displacement. The option to selectively accept initially less stable configurations ensures that the potential energy surface is fully sampled within the given stochastic constraints.

An excellent example of a Monte Carlo approach in molecular modeling is provided by Newsam et al. (1996) in their determination of the cation positions in zeolite materials. Knowledge of the positions of alkali metal cations in the aluminosilicate framework zeolites is vital to the design and control of the sorptive and catalytic properties of these industrially-important materials. X-ray diffraction determination of the optimal sites is often tedious and difficult due to the lack of quality single crystals, so the molecular simulation approach provides a convenient alternative. The simulation cell of the synthetic zeolite A ( $\text{NaSiAlO}_4$ ) is comprised of an equal amount of Al and Si atoms forming the framework structure having the characteristic zeolite rings and channels, and with twelve sodium ions counterbalancing the negative framework charge. The Monte Carlo packing simulation (Freeman et al. 1991) starts with a fixed framework and a potential energy surface defined by a set of Coulombic interactions and short-range interaction terms. Twelve Na ions are successively introduced into the framework structure ensuring that each new configuration leads to an acceptable energy via the scheme presented in Figure 11. Several thousand configuration attempts can be used to ensure that a statistically-sound sampling of the framework potential surface has been probed while avoiding any bias in identifying the Na ion sites. Further refinement of the thirty most favorable configurations was then performed using standard energy minimization techniques to arrive at eleven favorable configurations that agree with the experimental structure (Pluth and Smith 1980) having 8  $\text{Na}^+$  on the six-membered rings, 3  $\text{Na}^+$  on the eight-membered rings, and 1  $\text{Na}^+$  adjacent to one of the four-membered rings (see Fig. 12).

Similar Monte Carlo approaches have been successfully used to characterize the sorptive properties of zeolites for alkanes (Smit and Siepmann 1994; Smit 1995; Nascimento 1999; Suzuki et al. 2000), for aromatic organic compounds (Bremard et al. 1997; Klemm et al. 1998), for water (Channon et al. 1998), and for the sorption and transport rates of inorganic gases (Dougnet et al. 1996; Shen et al. 1999). Grand canonical methods are often implemented in these Monte Carlo studies to ensure a constant chemical potential  $\mu$  during the simulation. Use of the  $\mu VT$  ensemble allows for a computationally fast approach for attaining an equilibrium configuration, especially for a model that includes multiple phases such as the simulation of a gas or a fluid interacting with a solid. The temperature and chemical potential are externally imposed

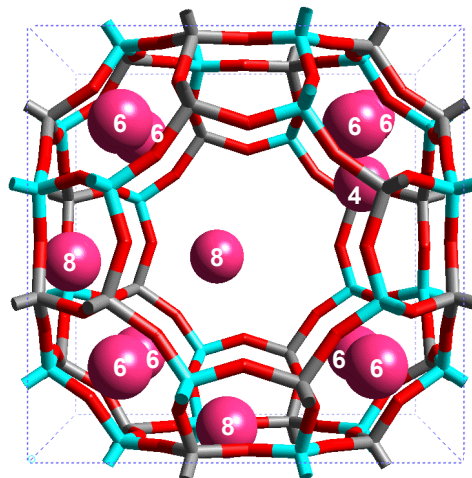


**Figure 12.** Perspective view of zeolite A showing one of the low energy configurations for the distribution of twelve Na ions within the structure as determined using a Monte Carlo sampling approach. The label on each Na ion represents the size of the Si-Al ring structure that the cation is associated with.

and the number of atoms or molecules is allowed to vary during the simulation. Details of grand canonical methods for use in Monte Carlo and molecular dynamics simulations are provided in Allen and Tildesley (1987) and Frenkel and Smit (1996). The extensive literature on the molecular simulation of zeolites attests to the vast number of industrial applications requiring unique catalysts, nanoporous materials, and molecular sieves.

Monte Carlo simulations have been similarly used to analyze the structure of species in the interlayer of clays. The structure and dynamics of interlayer water molecules and solvated cations are difficult to ascertain through conventional experimental and spectroscopic methods. In part, these difficulties are related to 1) their extremely fine grain size (typically less than 1  $\mu\text{m}$ ) of clay minerals; 2) their low crystallographic symmetry; 3) their complex chemistry with multiple components, cation disorder, and vacancies; and 4) the occurrence of stacking disorder that precludes long range ordering. Therefore, simulation methods, and, in particular, Monte Carlo techniques, are often used to develop a model for the detailed atomistic structure of the clay. Simulations of the swelling behavior of smectite clays have become quite commonplace in the mineralogical literature (e.g., Delville 1991; Skipper et al. 1991; Delville 1992; Beek et al. 1995; Chang et al. 1995; Delville 1995; Skipper et al. 1995a; Skipper et al. 1995b; Karaborni et al. 1996; Chang et al. 1997; Greathouse and Sposito 1998; Sposito et al. 1999). Recently, Sposito et al. (1999) determined the optimum positions of water molecules and cations in the expanded two layer hydrate of Na- and K-montmorillonite. The simulations involve several stages of generating acceptable Monte Carlo configurations based on the movement of water molecules, interlayer cations, and clay layers. The K-montmorillonite simulations required more than 1,700,000 steps to attain a data set suitable for evaluating the optimized configuration of interlayer water and cations. Radial distribution functions for interlayer water derived from their simulation results suggest a strong influence of the smectite tetrahedral sheets in modifying the tetrahedral coordination that exists in bulk water. This effect was more pronounced for the K-montmorillonite where the weak solvation of  $\text{K}^+$  is more readily influenced by the clay layers.

### **Molecular dynamics methods**

Molecular dynamics simulation is a deterministic technique to model the equilibrium and transport properties of a chemical system based on a set of interatomic potentials or forcefield terms. A large assemblage of atoms can be examined as either a cluster or periodic system whereby Newton's equations of motion involving forces and velocities are iteratively solved to provide a classical description for a many-body system, here comprised of atoms. A molecular dynamics simulation first requires the input of an initial configuration for the system with an assignment of a velocity for each of the atoms. Usually a Boltzmann distribution of velocities is initially imparted onto all or a subset of the atoms contained in the simulation cell. The velocities are then scaled to provide the appropriate mean kinetic energy for the system to meet the desired temperature. Forces are derived based on the given forcefield, and then the equations of motion are integrated over the selected time interval. Time increments, usually on the order of a femtosecond or less, are then chosen so that all atomic motions are resolvable for the time step (i.e., the time increment is significantly less than the period of any vibrational mode associated with the model). Typically, the Verlet algorithm (1967) or similar method is used to calculate the new atomic positions and velocities that are then used to loop through the integration for the next time step. The procedure is repeated for a large number of iterations, typically on the order of several hundred thousand times, allowing the system to evolve to an equilibrium configuration (tens to hundreds of picoseconds of simulation time). Values for the temperature, and potential and kinetic energies can be evaluated throughout the molecular dynamics simulation via instantaneous or running averages. An

NPT canonical ensemble (isobaric and isothermal with a constant number of atoms) can be used for the simulation of an unconstrained periodic system, allowing for the examination of the pressure and density of the simulation cell as a function of time. Allen and Tildesley (1987), Frenkel and Smit (Frenkel and Smit 1996), and Haile (1997) provide excellent descriptions of the procedures associated with a molecular dynamics simulation.

Molecular dynamics simulations overcome some of the limitations associated with energy minimization schemes by allowing the kinetic energy of the system to assist atoms in better sampling of the potential energy surface. In this respect, molecular dynamics comes closest to describing the many aspects of a real experiment. Although the goal of optimizing a molecular configuration through the static energy minimization approach is to attain the most stable configuration associated with the global energy minimum, the method does not allow one to monitor the evolution of the chemical system. Temperature is explicitly incorporated in a molecular dynamics simulation and the kinetic energy assists molecular and atomic motions to overcome potential energy barriers. Thermal annealing methods allow a wide range of potential molecular configurations that would be inaccessible through the standard energy minimization technique. Impulse dynamics methods are often used to direct the transport of atoms or molecules toward a reactive site or through a diffusion pathway. Additionally, thermodynamic integration and analysis of various ensemble averages at state points can be used to derive thermodynamic properties (Allen and Tildesley 1987). This is of particular significance for grand canonical ensembles, where estimates of Gibbs and Helmholtz free energies and entropy values can be derived.

Applications of molecular dynamics in mineralogy and geochemistry are often associated with the simulation of the structure and transport properties of fluids and melts due to the relatively rapid dynamics of the species in these systems. Melt and glass simulations (e.g., Kubicki and Lasaga 1988; Belonoshko and Dubrovinsky 1995; Stein and Spera 1995; Chaplot et al. 1998; Nevins and Spera 1998) have often provided atomistic details of mineral/melt systems at extreme conditions that are not necessarily observable under laboratory conditions. Fluid behavior at ambient, hydrothermal, and supercritical conditions have been successfully modeled using molecular dynamics simulations (e.g., Brodholt and Wood 1990, 1993; Duan et al. 1995; Kalinichev and Heinzinger 1995; Driesner et al. 1998; Driesner and Seward 2000). Although less amenable to the modeling technique due to the larger time scale associated with solids, molecular dynamics simulations of mantle phases have also helped to constrain phase transitions and their associated geophysical discontinuities (e.g., Matsui 1988; Miyamoto 1988; Matsui and Price 1992; Winkler and Dove 1992).

Similarly, the molecular dynamics method has been successfully used to evaluate the structure and dynamics of water, interlayer cations, and environmental contaminants in clays (e.g., Teppen et al. 1997; Hartzell et al. 1998; Smith 1998; Teppen et al. 1998; Kawamura et al. 1999), and water and interlayer anions in layered double hydroxides such as hydrotalcite and other related phases (Aicken et al. 1997; Kalinichev et al. 2000; Wang et al. 2001). An example of the use of molecular dynamics to examine the behavior of interlayer waters in clay minerals is provided in the recent study of Cygan et al. (2001). A smectite clay corresponding to a Na-montmorillonite composition was simulated using a fully flexible forcefield, developed for clays and hydrous minerals, in which all atoms of the simulation cell were free to translate during the simulation. An NPT canonical ensemble provided complete freedom of the clay layers to expand with the sequential addition of water molecules to the simulation cell. The anhydrous system was first equilibrated for 40 picoseconds using 1 femtosecond time steps, then a single water

molecule was added to the interlayer region of the smectite. Molecular dynamics was continued for 40 additional picoseconds before the addition of another water molecule and further equilibration, and so on until the smectite clay was expanded to more than 21 Å at a water content of 0.45 g H<sub>2</sub>O/g clay, corresponding to the addition of 73 water molecules to the clay interlayer.

Figure 13 presents the results of the mean basal d-spacing based on the last 20 picoseconds of simulation time for each smectite structure as a function of water content. The experimental water adsorption data for smectite (Fu et al. 1990; Berend et al. 1995) is also included to show the general agreement between the molecular dynamics simulation results and the experimental values. The fine detail of the expansion of the smectite layers is reproduced by the model as the first hydrate layer is introduced into the interlayer. The clay expands to approximately 12 Å with the initial introduction of water and stays approximately at that value as water molecules fill in the interlayer voids and fully solvate the interlayer Na cations. A critical water amount is met at approximately 0.14 g H<sub>2</sub>O/g clay (23 water molecules in simulation cell) where the smectite expands to approximately 15 Å with formation of the stable two-layer hydrate. Each expansion of the clay represents the critical point where the energy of the clay layer expansion overrides the energy gain in forming a hydrogen bonded water network in the interlayer. The molecular dynamics simulations provide a basis for the continued expansion of the smectite clay with the addition of more water molecules. However, further expansion of the Na-montmorillonite beyond the 15 Å two-layer hydrate is not observed in nature. Smith (1998) uses a molecular dynamics approach and the various representations of the hydration energy to demonstrate the relative stabilities of each of the stable hydration states for a Cs-montmorillonite. Grand canonical molecular dynamics and an analysis of the free energy of swelling were later used to confirm the stable clay hydration states (Shroll and Smith 1999).

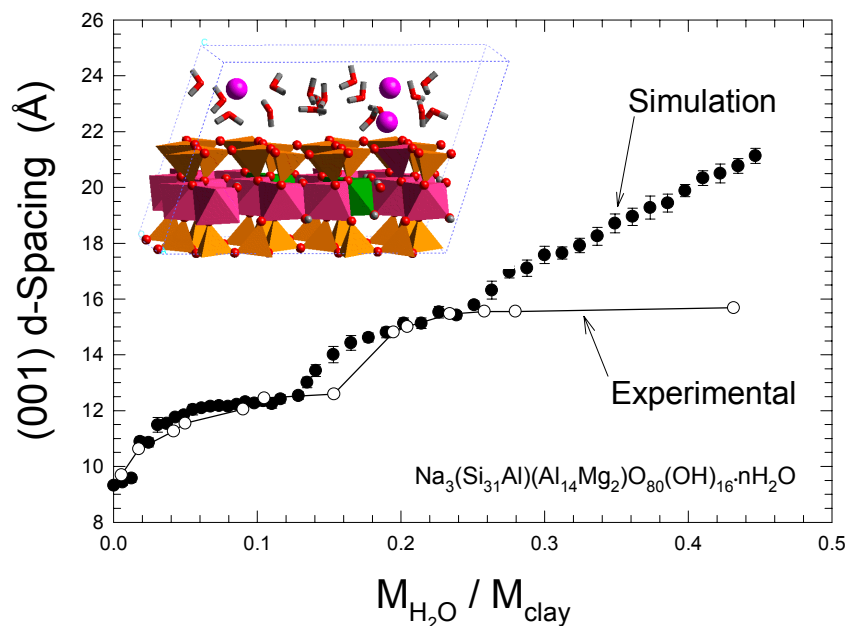


**Figure 13.** Swelling behavior for a smectite clay derived from molecular dynamics simulations of montmorillonite. The equilibrium d-spacing is presented as a function of water content of the clay. The plateaus in the experimental and simulation results at 12 Å and 15 Å represent the stabilization of, respectively, the one-layer (insert structure) and two-layer hydrates. No further expansion of the smectite is observed in nature beyond the two-layer hydrate. The simulations suggest that further swelling of the clay is possible although not thermodynamically favored.

## Quantum dynamics

Perhaps the ultimate molecular modeling method available to date is that of quantum dynamics, or *ab initio* molecular dynamics, in which molecular dynamics and quantum mechanics methods are combined. Simple classical-based forcefields and interaction parameters are replaced by the more complex quantum methods of Hartree-Fock and DFT to determine the energy and forces of interaction for the system. Rather than rely on simple interatomic potentials to describe the complex many-body interactions, quantum dynamics solves the Schrödinger equation for each dynamics time step to explicitly obtain the electronic structure for the entire system. This approach dispenses with the inherent limitations of the empirical method for deriving interaction parameters and the uncertainty associated with knowing the range of validity. Furthermore, quantum dynamics allows a closer match to reality where the electronic properties and atomic dynamics are dependent. This is especially critical for reactive systems where dissociation and bond formation occurs on the time scale of the simulation. The quantum dynamics approach was first pioneered by Car and Parinello (1985; 1987) by combining accurate DFT methods with dynamics to examine the equilibrium structure of melts and amorphous semiconductors. As expected, due to the high computational cost of performing these simulations, most quantum dynamics studies are limited to short simulation times (on the order of one to two picoseconds) and relatively small simulation cells. An example of the technique as applied to silicon surfaces is presented in Terakura et al. (1997) while Radeke and Carter (1997) provide a review of molecule-surface interactions. A recent comprehensive review of quantum dynamics methods is provided by Tuckerman (2000).

Although less common in the geosciences literature, quantum dynamics methods have been successfully used to examine the stabilities of potential phases of the lower mantle. The stability limits of  $\text{MgSiO}_3$  perovskite were derived by an optimization scheme using quantum dynamics with the local density approximation by Wentzcovitch (1993). Their simulations suggested the stability of the orthorhombic perovskite relative to the cubic phase increased with pressure (up to 150 GPa). The modeling approach was later used to examine the stability of the  $\text{MgSiO}_3$  ilmenite phase (Karki et al. 2000). The simulations suggested that the ilmenite phase would transform to the perovskite phase at 30 GPa. Haiber et al. (1997) examined the various phases of  $\text{Mg}_2\text{SiO}_4$  (olivine and spinel polymorphs) and analyzed the dynamics of a sorbed proton at elevated temperatures (400 to 1600 K). Recently, in an application related to catalysis and environmental concerns, Hass et al. (1998) examined the dissociation of water on hydrated alumina surfaces. The quantum dynamics studies examined a relatively large simulation cell comprised of 135 atom alumina substrate that was subsequently hydrated at two different water coverages. The simulations indicated, within the one picosecond simulation time, water dissociation and proton transfer reactions between the adsorbed molecular water and the hydroxide surface. Similarly, Lubin et al. (2000) successfully used quantum dynamics to examine the solvation of hydrolyzed aluminum ions in water clusters and determine the mechanisms of proton transfer.

## FORSTERITE: THE VERY MODEL OF A MODERN MAJOR MINERAL

The crystal structure and physical properties of forsterite ( $\text{Mg}_2\text{SiO}_4$ ) have been determined by a variety of molecular modeling methods and therefore are represented by a fair number of papers in the mineralogical literature. Forsterite, as the magnesium endmember of the orthosilicate olivine series, is the most abundant phase of the upper mantle of the Earth. The elastic properties of forsterite are expected to control the rheology of this region (Evans and Dresen 1991; Duffy and Ahrens 1992) and will

influence plate tectonic processes of the crust, while the electrical conductivity of forsterite is critical to field investigations involving geomagnetic and magnetotelluric surveys (e.g., Jones 1999; Neal et al. 2000). The crystal structure of forsterite is depicted in Figure 14. This energy-optimized structure was obtained using a Buckingham potential with the partial charges and interaction parameters of Teter (2000) while maintaining orthorhombic *Pbnm* symmetry during the optimization. Cell parameters and Mg-O and Si-O bond lengths are in excellent agreement with the experimental structure (Fujino et al. 1981).

### Static calculations and energy minimization studies

Early models of forsterite relied on classical molecular modeling methods to describe the interaction of ions using formal charges for the Coulombic interactions and empirically-derived parameters for the short-range interactions. Static energy calculations and energy minimization techniques were used to evaluate and optimize Mg-O and Si-O bond lengths and cell lengths of the orthorhombic unit cell. Lasaga (1980), Post and Burnham (1986), and Catti (1989) developed models that successfully mimicked the observed crystallographic structure of forsterite. Similarly, Matsui and Busing (1984) accurately modeled the forsterite structure but used a set of potentials based on Mg ions and rigid  $\text{SiO}_4^{4-}$  groups (Matsui and Matsumoto 1982). The Catti model and Matsui and Busing models both provided reasonable values for the elastic properties of forsterite derived from the second derivatives of the energy matrix for the optimized structure. The Lasaga approach evaluated the point defect structure of forsterite and successfully predicted the anisotropic behavior of Mg diffusion (Lasaga 1980). An evaluation of cation site preference energies (M1 *versus* M2 octahedral site) for various endmember compositions of olivine was completed by Bish and Burnham (1984) using a combined approach of distance-least-squares method of structural analysis and lattice energy calculations. More recently, a molecular mechanics method was used to evaluate the surface structure and energies of forsterite (Watson et al. 1997). Surface energies obtained in the analysis of the various relaxed surfaces provided an accurate model of the crystal morphology.

### Lattice dynamics studies

Lattice dynamics modeling of forsterite has provided significant new insights into the dynamical nature of a complex silicate structure and the link between atomistic structure and macroscopic thermodynamics. Lattice dynamics methods examine the interaction of lattice vibrations as weakly interacting phonons; a phonon being a particle representation of low frequency sound waves. Basically, a lattice dynamical model for a crystal is represented by a tensor that combines the coupling between forces and atomic displacements. Born and Huang (1954) and Wallace (1972) provide excellent comprehensive discussions of the basic theory of lattice dynamics. Combined with inelastic neutron scattering experiments,

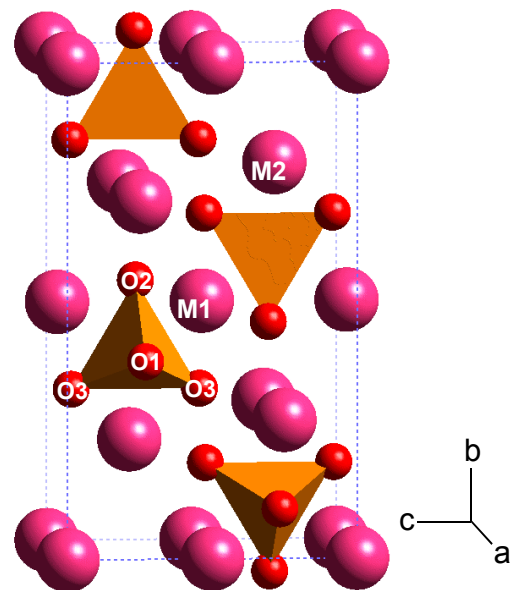


**Figure 14.** Energy-optimized structure of the orthorhombic unit cell of forsterite ( $\text{Mg}_2\text{SiO}_4$ ) obtained with an ionic model. Magnesium sites M1 and M2 and the silicon tetrahedron with O1, O2, and two O3 oxygens comprise the asymmetric unit.

lattice dynamics provides a powerful tool for evaluating phonon dispersion, vibrational energies, and thermodynamic properties such as heat capacity and entropy. Early attempts by Iishi (1978) and Kieffer (1980) were successful in predicting the temperature dependence of the heat capacity and the vibrational spectrum for forsterite. Besides providing a strong theoretical basis for the experimental calorimetric studies on minerals in the 1970's (e.g., Robie et al. 1978), this early theoretical work pioneered the way for more accurate lattice dynamics simulations of forsterite and related phases (e.g., Price et al. 1987; Rao et al. 1988; Patel et al. 1991; Kubicki and Lasaga 1992).

### Quantum studies

Quantum methods were first applied in the theoretical analysis of forsterite in the 1990's due to the advances in computer processors and development of efficient quantum software programs for periodic systems. Computer technology had matured so that it was finally possible to routinely calculate the electronic structure of complex minerals using sophisticated quantum chemistry tools. A Hartree-Fock pseudopotential method was used by Silvi et al. (1993) to evaluate the relative energies of the  $\text{Mg}_2\text{SiO}_4$  polymorphs and the local bonding environments. Brodholt et al. (1996) used a DFT approach and local density approximation to optimize the forsterite structure and to ascertain the compressional behavior of the phase up to 70 GPa. Wentzcovitch and Stixrude (1997) determined that the Mg octahedra and Si tetrahedra in forsterite compress nearly isotropically for pressures up to 25 GPa. They used the local density approximation and DFT method, in combination with a modified molecular dynamics approach, to obtain the optimized structure of forsterite at each pressure. The modeling results were in agreement with those of Brodholt et al. (1996) and confirmed that forsterite did not experience any changes in compression mechanism with pressure. This suggests the possibility that compression changes in the pressure medium, rather than in the forsterite crystal, were being measured in the experimental study (Kudoh and Takeuchi 1985).

More sophisticated calculations of forsterite using a DFT approach with the generalized gradient approximation were recently reported by Brodholt (1997) and Winkler et al. (1996). The former study examined the energetics of various Mg and O defects in forsterite and determined that Mg diffusion was dominated by a diffusion pathway involving jumps between M1 sites. The results are in agreement with the classical approach used by Lasaga (1980) as discussed previously. The Winkler et al. (1996) study used the non-local DFT approach to obtain the electric field gradient tensors associated with NMR active nuclei in forsterite ( $^{25}\text{Mg}$  and  $^{17}\text{O}$ ).

## THE FUTURE

Molecular modeling has come a long way since John Dalton first used wooden balls in the early nineteenth century to represent molecular structures. Rapid changes in computer technologies and hardware, the introduction of the personal computer, the development of massively-parallel supercomputers, the use of new and efficient algorithms and visually-based programming, the intelligence of neural networks, and the ability of the internet to distribute complex computational problems across thousands, if not potentially millions of networked computers, have all influenced the rapid growth of computational chemistry over the last two decades. How further technological developments will affect how we do molecular modeling in the geosciences on larger and more complex chemical systems is uncertain. However, it is certain that molecular modeling theory and computational methods will play a more significant role in how mineralogists and geochemists examine the complex phases and processes of the Earth.

## ACKNOWLEDGMENTS

The content of this chapter benefited from discussions and reviews provided by James Kubicki, David Teter, and Henry Westrich. The author is appreciative of funding provided by the U.S. Department of Energy, Office of Basic Energy Sciences, Geosciences Research and the U.S. Nuclear Regulatory Commission, Office of Nuclear Regulatory Research. Sandia is a multiprogram laboratory operated by Sandia Corporation, a Lockheed Martin company, for the United States Department of Energy under contract DE-AC04-94AL85000. Additionally, the author is extremely grateful to the many students, post-docs, colleagues, and collaborators who have contributed to the research efforts in using molecular simulations to understand the complex nature of minerals and geochemical systems.

## GLOSSARY OF TERMS

- Ab initio**—First principles quantum mechanical approach for obtaining the electronic properties of a molecule based on the approximate solutions to the many-electron Schrödinger equation, using only fundamental constants, and the mass and charge of the nuclear particles; literally “from the beginning”.
- Basis function**—Functions describing the atomic orbitals that when linearly combined make up the set of molecular orbitals in a quantum mechanics calculation; Gaussian basis sets and Slater type orbitals are examples of basis functions.
- Born-Oppenheimer approximation**—A method for separating electronic motion from that of the nuclei in quantum mechanics; the nuclei having greater mass are assumed stationary while the electrons are moving around them.
- Buckingham potential**—Function used for describing the energy of the Coulombic and short-range interactions of ionic or partially-ionic compounds; incorporates a two-parameter exponential and one-parameter dispersion term.
- Correlation energy**—The difference between the experimental energy and the Hartree-Fock energy in quantum mechanics; related to the neglect of local distortion in the distribution of electrons in the calculation.
- Coulombic energy**—The energy associated with the electrostatic force between two charged bodies (atoms or ions) that is inversely proportional to the distance separating the two charges; like sign charges repulse each other (positive potential energy) while opposite sign charges attract (negative potential energy).
- Density functional theory**—Class of quantum methods in which the total energy is expressed as a function of the electron density, and which the exchange and correlation contributions are based on the solution of the Schrödinger equation for an electron gas.
- Electron density**—Function that provides the number of electrons per volume of space.
- Electrostatic potential**—Function describing the energy of interaction for a positive point charge interacting with the nuclei and, in quantum mechanics, the electrons of a molecular system.
- Energy minimization**—Computational procedure for altering the configuration of a molecular model until the minimum energy arrangement has been attained. Approach is used in molecular dynamics, Monte Carlo simulation, and quantum mechanics methods.
- Forcefield**—A set of parameterized analytical expressions used in molecular mechanics for evaluating the contributions to the total potential energy of a molecular system; forcefields typically, but not always, include contributions for bond stretching, angle bending, dihedral torsion, van der Waals, and Coulombic interactions.
- Frontier orbital**—Concept of molecular reactivity in quantum mechanics involving the location of the largest electron density associated with the HOMO and LUMO of the molecule.
- Hamiltonian**—Operator function that describes the total energy of a molecule; operates on the wavefunction, and is part of the Schrödinger equation.

- Hartree-Fock method**—Quantum mechanics approach that computes the energy of a molecular system with a single determinant wavefunction; a trial wavefunction is iteratively improved until self consistency is attained.
- Hessian**—A matrix of second derivatives of the energy (force constants) with respect to the atomic coordinates of the molecular system; Hessian can be derived from various molecular mechanics and quantum mechanics approaches.
- HOMO**—Highest occupied molecular orbital in a quantum mechanics calculation.
- Kohn-Sham equations**—Quantum mechanics approach used for expressing the energy of a multi-electron system as a function of electron density; basis of density functional theory.
- Lattice dynamics**—Statistical mechanics approach for evaluating the vibrational frequencies (phonons) of a material based on classical mechanics and assuming harmonic vibrational modes; useful for the derivation of phonon dispersion curves and thermodynamic properties.
- LCAO**—Linear combination of atomic orbitals; method used in Hartree-Fock methods to describe multi-electron molecular wavefunctions.
- LUMO**—Lowest unoccupied molecular orbital in a quantum mechanics calculation.
- Molecular mechanics**—Molecular modeling method based on the empirical parameterization of analytical expressions to describe the energy of a molecular system in terms of various energy components (e.g., Coulombic, van der Waals, bond stretch, angle bend, etc.).
- Molecular dynamics**—Deterministic molecular modeling tool that evaluates the forces on individual atoms using an energy forcefield, then uses Newton's classical equation of motion to compute new atomic positions after a short time interval (on the order of a femtosecond); successive evaluation for a large number of time steps provides a time-dependent trajectory of all atomic motions.
- Molecular orbital**—Quantum mechanics function, comprised of atomic-based basis functions, for describing the delocalized nature of electrons in a molecule.
- Monte Carlo simulation**—A stochastic modeling method for obtaining optimized molecular structures and configurations based on the analysis of a large number of randomly-generated trial configurations.
- Quantum mechanics**—Molecular modeling method that examines the electronic structure and energy of molecular systems based on various schemes for solving the Schrödinger equation; based on the quantized nature of electronic configurations in atomic and molecular orbitals.
- Self-consistent field**—Iterative method used in quantum mechanics to obtain refinements to various approximations for solving the Schrödinger equation; a SCF calculation is complete when the molecular orbitals and energy are identical to those obtained in the preceding step.
- Semi-empirical**—Methods used in quantum mechanics to obtain approximate solutions to the Schrödinger equation by incorporating empirical parameters.
- Van der Waals energy**—Energy associated with the short-range interactions between closed-shell molecules; includes attractive forces involving interactions between the partial electric charges, and repulsive forces from the Pauli exclusion principle and the exclusion of electrons in overlapping orbitals.
- Wavefunction**—Eigenvector result from the Schrödinger wave equation that describes the dynamical properties of a molecular system.

## REFERENCES

- Agnon A, Bukowinski MST (1990) Thermodynamic and elastic properties of a many-body model for simple oxides. *Phys Rev B: Condens Matter* 41:7755-7766
- Aicken AM, Bell IS, Coveney PV, Jones W (1997) Simulation of layered double hydroxide intercalates. *Adv Mater* 9:496-500
- Allen MP, Tildesley DJ (1987) *Computer Simulation of Liquids*. Oxford University Press, Oxford
- Bader RFW (1990) *Atoms in Molecules*, vol 22. Oxford University Press, Oxford
- Baker J (1993) Techniques for geometry optimization: A comparison of Cartesian and natural internal coordinates. *J Comput Chem* 14:1085-1100

- Beek ES, Coveney PV, Skipper NT (1995) Monte Carlo molecular modeling studies of hydrated Li-smectites, Na-smectites, and K-smectites: Understanding the role of potassium as a clay swelling inhibitor. *J Am Chem Soc* 117:12608-12617
- Belonoshko AB, Dubrovinsky LS (1995) Molecular dynamics of stishovite melting. *Geochim Cosmochim Acta* 59:1883-1889
- Berend I, Cases JM, Francois M, Uriot JP, Michot L, Masion A, Thomas F (1995) Mechanism of adsorption and desorption of water vapor by homoionic montmorillonites: 2. The Li<sup>+</sup>, Na<sup>+</sup>, K<sup>+</sup>, Rb<sup>+</sup> and Cs<sup>+</sup>-exchanged forms. *Clays Clay Miner* 43:324-336
- Billing GD (2000) Dynamics of Molecular Surface Interactions. John Wiley and Sons, New York
- Bish DL, Burnham CW (1984) Structure energy calculations on optimum distance model structures: Application to the silicate olivines. *Am Mineral* 69:1102-1109
- Born M, Huang K (1954) Dynamical Theory of Crystal Lattices. Oxford University Press, London
- Bremard C, Buntinx G, Ginestet G (1997) Vibrational studies and Monte Carlo simulations of the sorption of aromatic carbonyls in faujasitic zeolites. *J Mol Struct* 410:379-382
- Breneman CM, Wiberg KB (1990) Determining atom-centered monopoles from molecular electrostatic potentials: The need for high sampling density in formamide conformational analysis. *J Comput Chem* 11:361-373
- Brodholt J (1997) *Ab initio* calculations on point defects in forsterite (Mg<sub>2</sub>SiO<sub>4</sub>) and implications for diffusion and creep. *Am Mineral* 82:1049-1053
- Brodholt J, Patel A, Refson K (1996) An *ab initio* study of the compressional behavior of forsterite. *Am Mineral* 81:257-260
- Brodholt J, Wood B (1990) Molecular dynamics of water at high temperatures and pressures. *Geochim Cosmochim Acta* 54:2611-2616
- Brodholt J, Wood B (1993) Molecular dynamics simulations of the properties of CO<sub>2</sub>-H<sub>2</sub>O mixtures at high pressures and temperatures. *Am Mineral* 78:558-564
- Busing WR (1970) An interpretation of the structures of alkaline earth chlorides in terms on interionic forces. *Trans Am Cryst Assoc* 6:57-72
- Caillol JM, Levesque D (1991) Numerical simulations of homogeneous and inhomogeneous ionic systems: An efficient alternative to the Ewald method. *J Chem Phys* 94:597-607
- Car R, Parrinello M (1985) Unified approach for molecular dynamics and density functional theory. *Phys Rev Lett* 55:2471-2474
- Car R, Parrinello M (1987) The unified approach to density functional and molecular dynamics in real space. *Solid State Commun* 62:403-405
- Catlow CRA, Faux ID, Norgett MJ (1976) Shell and breathing shell model calculations for defect formation energies and volumes in magnesium oxide. *J Phys C: Solid State Phys* 9:419-429
- Catlow CRA, Thomas JM, Parker SC, Jefferson DA (1982) Simulating silicate structures and the structural chemistry of pyroxenoids. *Nature* 295, no. 5851:658-662
- Catti M (1989) Modeling of structural and elastic changes of forsterite (Mg<sub>2</sub>SiO<sub>4</sub>) under stress. *Phys Chem Miner* 16:582-590
- Chang FC, Skipper NT, Sposito G (1995) Computer simulation of interlayer molecular structure in sodium montmorillonite hydrates. *Langmuir* 11:2734-2741
- Chang FC, Skipper NT, Sposito G (1997) Monte Carlo and molecular dynamics simulations of interfacial structure in lithium-montmorillonite hydrates. *Langmuir* 13:2074-2082
- Channon YM, Catlow CRA, Gorman AM, Jackson RA (1998) Grand canonical Monte Carlo investigation of water adsorption in heulandite-type zeolites. *J Phys Chem B* 102:4045-4048
- Chaplot SL, Choudhury N, Rao KR (1998) Molecular dynamics simulation of phase transitions and melting in MgSiO<sub>3</sub> with the perovskite structure. *Am Mineral* 83:937-941
- Chirlian LE, Francl MM (1987) Atomic charges derived from electrostatic potentials: A detailed study. *J Comput Chem* 8:894-905
- Clark T (1985) A Handbook of Computational Chemistry: A Practical Guide to Chemical Structure and Energy Calculations. John Wiley and Sons, New York
- Cohen RE (1991) Bonding and elasticity of stishovite SiO<sub>2</sub> at high pressure: Linearized augmented plane-wave calculations. *Am Mineral* 76:733-742
- Coles ME, Hazlett RD, Spanne P, Soll WE, Muegge EL, Jones KW (1998) Pore level imaging of fluid transport using synchrotron X-ray microtomography. *J Petrol Sci Eng* 19:55-63
- Cook DB (1998) Handbook of Computational Quantum Chemistry. Oxford University Press, Oxford
- Coppens P (1992) Electron density from X-ray diffraction. *Annu Rev Phys Chem* 43:663-692
- Cygan RT, Liang J-J, Kalinichev AG (2001) Molecular models of hydroxide, oxyhydroxide, and clay phases and the development of a general forcefield. *J Phys Chem*:submitted

- Dauber-Osguthorpe P, Roberts VA, Osguthorpe DJ, Wolff J, Genest M, Hagler AT (1988) Structure and energetics of ligand-binding to proteins: Escherichia-coli dihydrofolate reductase trimethoprim, a drug-receptor system. *Proteins: Struct Funct Genet* 4:31-47
- de Leeuw SW, Perram JW, Smith ER (1980) Simulation of electrostatic systems in periodic boundary conditions: 1. Lattice sums and dielectric constants. *Proc R Soc London, A* 373:27-56
- Delley B (1990) An all-electron numerical method for solving the local density functional for polyatomic molecules. *J Chem Phys* 92:508-517
- Delville A (1991) Modeling the clay-water interface. *Langmuir* 7:547-555
- Delville A (1992) Structure of liquids at a solid interface: An application to the swelling of clay by water. *Langmuir* 8:1796-1805
- Delville A (1995) Monte Carlo simulations of surface hydration: An application to clay wetting. *J Phys Chem* 99:2033-2037
- Dick BG, Overhauser AW (1958) Theory of the dielectric constants of alkali halide crystals. *Phys Rev* 112:90-103
- Douguet D, Pellenq RJM, Boutin A, Fuchs AH, Nicholson D (1996) The adsorption of argon and nitrogen in silicalite-1 zeolite: A grand canonical Monte-Carlo study. *Mol Sim* 17:255-288
- Driesner T, Seward TM (2000) Experimental and simulation study of salt effects and pressure/density effects on oxygen and hydrogen stable isotope liquid-vapor fractionation for 4-5 molal aqueous NaCl and KCl solutions to 400 degrees C. *Geochim Cosmochim Acta* 64:1773-1784
- Driesner T, Seward TM, Tironi IG (1998) Molecular dynamics simulation study of ionic hydration and ion association in dilute and 1 molal aqueous sodium chloride solutions from ambient to supercritical conditions. *Geochim Cosmochim Acta* 62:3095-3107
- Duan ZH, Moller N, Weare JH (1995) Molecular dynamics equation of state for nonpolar geochemical fluids. *Geochim Cosmochim Acta* 59:1533-1538
- Duffy TS, Ahrens TJ (1992) Sound velocities at high pressure and temperature and their geophysical implications. *J Geophys Res, Solid Earth* 97:4503-4520
- Evans B, Dresen G (1991) Deformation of Earth materials: 6 easy pieces. *Rev Geophys* 29:823-843
- Ewald PP (1921) Die Berechnung optischer und elektrostatischer Gitterpotentiale. *Annalen der Physik* 64:253-287
- Fischer TH, Almlöf J (1992) General methods for geometry and wave function optimization. *J Phys Chem* 96:9768-9774
- Flekkoy EG, Coveney PV (1999) From molecular dynamics to dissipative particle dynamics. *Phys Rev Lett* 83:1775-1778
- Freeman CM, Catlow CRA, Thomas JM, Brode S (1991) Computing the location and energetics of organic-molecules in microporous adsorbents and catalysts: A hybrid approach applied to isomeric butenes in a model zeolite. *Chem Phys Lett* 186:137-142
- Frenkel D, Smit B (1996) *Understanding Molecular Simulation*. Academic Press, San Diego
- Fu MH, Zhang ZZ, Low PF (1990) Changes in the properties of a montmorillonite-water system during the adsorption and desorption of water: Hysteresis. *Clays Clay Miner* 38:485-492
- Fujino K, Sasaki S, Takeuchi Y, Sadanaga R (1981) X-ray determination of electron distributions in forsterite, fayalite and tephroite. *Acta Crystallogr, Sect B: Struct Sci* 37:513-518
- Gibbs GV (1982) Molecules and models for bonding in silicates. *Am Mineral* 67:421-450
- Gibbs GV, Hamil MM, Louisnathan SJ, Bartell LS, Yow H (1972) Correlations between Si-O bond length, Si-O-Si angle and bond overlap populations calculated using extended Huckel molecular orbital theory. *Am Mineral* 57:1578-1613
- Gill PMW, Johnson BG, Pople JA, Frisch MJ (1992) An investigation of the performance of a hybrid of Hartree-Fock and density functional theory. *Int J Quantum Chem* S26:319-331
- Gillan MJ, Lindan PJD, Kantorovich LN, Bates SP (1998) Molecular processes on oxide surfaces studied by first-principles calculations. *Mineral Mag* 62:669-685
- Greathouse J, Sposito G (1998) Monte Carlo and molecular dynamics studies of interlayer structure in Li(H<sub>2</sub>O)<sub>3</sub>-smectites. *J Phys Chem B* 102:2406-2414
- Greengard L, Rokhlin V (1987) A fast algorithm for particle simulations. *J Comput Phys* 73:325-348
- Haiber M, Ballone P, Parrinello M (1997) Structure and dynamics of protonated Mg<sub>2</sub>SiO<sub>4</sub>: An *ab initio* molecular dynamics study. *Am Mineral* 82:913-922
- Haile JM (1997) *Molecular Dynamics Simulation: Elementary Methods*. John Wiley and Sons, New York
- Hartzell CJ, Cygan RT, Nagy KL (1998) Molecular modeling of the tributyl phosphate complex of europium nitrate in the clay hectorite. *J Phys Chem A* 102:6722-6729
- Hass KC, Schneider WF, Curioni A, Andreoni W (1998) The chemistry of water on alumina surfaces: Reaction dynamics from first principles. *Science* 282:265-268
- Hazen RH (1976) Effects of temperature and pressure on the cell dimension and X-ray temperature factors of periclase. *Am Mineral* 61:266-271

- Hehre WJ (1995) Practical Strategies for Electronic Structure Calculations. Wavefunction, Irvine
- Hehre WJ, Radom L, Schleyer PvR, Pople JA (1986) *Ab initio* Molecular Orbital Theory. John Wiley and Sons, New York
- Hehre WJ, Stewart RF, Pople JA (1969) Self-consistent molecular-orbital methods. I. Use of Gaussian expansions of Slater-type atomic orbitals. *J Chem Phys* 51:2657-2664
- Hohenberg P, Kohn W (1964) Density functional theory of the inhomogeneous electron gas. *Phys Rev* B136:864-871
- Iishi K (1978) Lattice dynamics of forsterite. *Am Mineral* 63:1198-1208
- Jackson RA, Catlow CRA (1988) Computer simulation of zeolite structure. *Mol Sim* 1:207-224
- Jones AG (1999) Imaging the continental upper mantle using electromagnetic methods. *Lithos* 48:57-80
- Jones RO, Gunnarsson O (1989) The density functional formalism, its applications and prospects. *Rev Mod Phys* 61:689-746
- Kalinichev AG, Heinzinger K (1995) Molecular dynamics of supercritical water: A Computer simulation of vibrational spectra with the flexible BJH potential. *Geochim Cosmochim Acta* 59:641-650
- Kalinichev AG, Kirkpatrick RJ, Cygan RT (2000) Molecular modeling of the structure and dynamics of the interlayer and surface species of mixed-metal layered hydroxides: Chloride and water in hydrocalumite (Friedel's Salt). *Am Mineral* 85:1046-1052
- Karaborni S, Smit B, Heidug W, Urai J, Oort v (1996) The swelling of clays: Molecular simulations of the hydration of montmorillonite. *Science* 271:1102-1104
- Karki BB, Duan W, DaSilva CRS, Wentzcovitch RM (2000) *Ab initio* structure of MgSiO<sub>3</sub> ilmenite at high pressure. *Am Mineral* 85:317-320
- Kawamura K, Ichikawa Y, Nakano M, Kitayama K, Kawamura H (1999) Swelling properties of smectite up to 90 degrees C: *In situ* X-ray diffraction experiments and molecular dynamic simulations. *Eng Geol* 54:75-79
- Kendrew JC, Bodo G, Dintzis HM, Parrish RG, Wyckoff H, Phillips DC (1958) A three-dimensional model of the myoglobin molecule obtained by X-ray analysis. *Nature* 181:662-666
- Kieffer SW (1980) Thermodynamics and lattice vibrations of minerals: 4. Application to chain and sheet silicates and orthosilicates. *Rev Geophys* 18:862-886
- Klemm E, Wang JG, Emig G (1998) A comparative study of the sorption of benzene and phenol in silicalite: HAlZSM-5 and NaAlZSM-5 by computer simulation. *Micropor Mesopor Mat* 26:11-21
- Kohn W, Sham LJ (1965) Self-consistent equations including exchange and correlation effects. *Phys Rev* 140:1133-1138
- Kubicki JD, Lasaga AC (1988) Molecular dynamics simulations of SiO<sub>2</sub> melt and glass: Ionic and covalent models. *Am Mineral* 73:941-955
- Kubicki JD, Lasaga AC (1992) *Ab initio* molecular dynamics simulations of melting in forsterite and MgSiO<sub>3</sub> perovskite. *Am J Sci* 292:153-183
- Kudoh Y, Takeuchi Y (1985) The crystal structure of forsterite Mg<sub>2</sub>SiO<sub>4</sub> under high pressure up to 149 kb. *Z Kristallogr* 171:291-302
- Labanowski JK, Andzelm JW (1991) *Density Functional Methods in Chemistry*. Springer-Verlag, New York
- Lasaga AC (1980) Defect calculations in silicates: Olivine. *Am Mineral* 65:1237-1248
- Lasaga AC (1992) *Ab initio* methods in mineral surface reactions. *Rev Geophys* 30:269-303
- Leach AR (1996) *Molecular Modeling Principles and Applications*. Addison Wesley Longman Limited, Essex
- Levinthal C (1966) Molecular model-building by computer. *Sci Am* 214:42-52
- Lewis GV, Catlow CRA (1986) Potential models for ionic oxides. *J Phys C: Solid State Phys* 18:1149-1161
- Lifson S, Warshel A (1968) Consistent force field for calculations of conformations, vibrational Spectra and enthalpies of cycloalkane and n-alkane molecules. *J Chem Phys* 49:5116-5129
- Lubin MI, Bylaska EJ, Weare JH (2000) *Ab initio* molecular dynamics simulations of aluminum ion solvation in water clusters. *Chem Phys Lett* 322:447-453
- Matsui M (1988) Molecular dynamics study of MgSiO<sub>3</sub> perovskite. *Phys Chem Miner* 16:234-238
- Matsui M, Busing WR (1984) Computational modeling of the structure and elastic constants of the olivine and spinel forms of Mg<sub>2</sub>SiO<sub>4</sub>. *Phys Chem Miner* 11:55-59
- Matsui M, Matsumoto T (1982) An interatomic potential-function model for Mg, Ca and CaMg olivines. *Acta Crystallogr, Sect A: Found Crystallogr* 38:513-515
- Matsui M, Price GD (1992) Computer simulation of the MgSiO<sub>3</sub> polymorphs. *Phys Chem Miner* 18:365-372
- Metropolis N, Rosenbluth AW, Rosenbluth MN, Teller AH, Teller E (1953) Equation of state calculations by fast computing machines. *J Chem Phys* 21:1087-1092

- Milman V, Winkler B, White JA, Pickard CJ, Payne MC, Akhmatkaya EV, Nobes RH (2000) Electronic structure, properties, and phase stability of inorganic crystals: A pseudopotential plane-wave study. *Int J Quantum Chem* 77:895-910
- Miyamoto M (1988) Ion migration in MgSiO<sub>3</sub>-perovskite and olivine by molecular dynamics calculations. *Phys Chem Miner* 15:601-604
- Mulliken RS (1955) Electronic population analysis on LCAO-MO molecular wave functions. *J Chem Phys* 23:1833-1846
- Nascimento MAC (1999) Computer simulations of the adsorption process of light alkanes in high-silica zeolites. *Theochem* 464:239-247
- Neal SL, Mackie RL, Larsen JC, Schultz A (2000) Variations in the electrical conductivity of the upper mantle beneath North America and the Pacific Ocean. *J Geophys Res, Solid Earth* 105:8229-8242
- Nevins D, Spera FJ (1998) Molecular dynamics simulations of molten CaAl<sub>2</sub>Si<sub>2</sub>O<sub>8</sub>: Dependence of structure and properties on pressure. *Am Mineral* 83:1220-1230
- Newsam JM, Freeman CM, Gorman AM, Vessal B (1996) Simulating non-framework cation location in aluminosilicate zeolites. *Chem Comm* 16:1945-1946
- Olyphant N, Bartlett RJ (1994) A systematic comparison of molecular properties obtained using Hartree-Fock, a hybrid Hartree-Fock density functional theory, and coupled-cluster methods. *J Chem Phys* 100:6550-6561
- Patel A, Price GD, Mendelsohn MJ (1991) A computer simulation approach to modeling the structure, thermodynamics and oxygen isotope equilibria of silicates. *Phys Chem Miner* 17:690-699
- Payne MC, Teter MP, Allan DC, Arias TA, Joannopoulos JD (1992) Iterative minimization techniques for *ab initio* total-energy calculations: Molecular dynamics and conjugate gradients. *Rev Mod Phys* 64:1045-1097
- Perdew JP, Burke K, Ernzerhof M (1996) Generalized gradient approximation made simple. *Phys Rev Lett* 77:3865-3868
- Pluth JJ, Smith JV (1980) Accurate redetermination of crystal structure of dehydrated Zeolite-A: Absence of near zero coordination of sodium: Refinement of Si,Al-ordered superstructure. *J Am Chem Soc* 102:4704-4708
- Pople JA, Beveridge DL (1970) *Approximate Molecular Orbital Theory*. McGraw-Hill, New York
- Post JE, Burnham CW (1986) Ionic modeling of mineral structures and energies in the electron gas approximation: TiO<sub>2</sub> polymorphs, quartz, forsterite, diopside. *Am Mineral* 71:142-150
- Price GD, Parker SC, Leslie M (1987) The lattice dynamics of forsterite. *Mineral Mag* 51:157-170
- Radeke MR, Carter EA (1997) *Ab initio* dynamics of surface chemistry. *Annu Rev Phys Chem* 48:243-270
- Rao KR, Chaplot SL, Choudhury N, Ghose S, Hastings JM, Corliss LM, Price DL (1988) Lattice dynamics and inelastic neutron scattering from forsterite, Mg<sub>2</sub>SiO<sub>4</sub>: Phonon dispersion relation, density of states and specific heat. *Phys Chem Miner* 16:83-97
- Rappé AK, Goddard WA (1991) Charge equilibration for molecular dynamics simulations. *J Phys Chem* 95:3358-3363
- Robie RA, Hemingway BS, Fisher JR (1978) *Thermodynamic Properties of Minerals and related Substances at 298.15 K and 1 Bar (10<sup>5</sup> Pascals) Pressure and at Higher Temperatures*, vol 1452, Washington DC
- Rouvray DH (1997) Do molecular models accurately reflect reality? *Chem Ind* 15:587-590
- Rouvray DH (1995) John Dalton: The world's first stereochemist. *Endeavour* 19:52-57
- Schleyer PVR (1998) *Encyclopedia of Computational Chemistry*. John Wiley and Sons, New York
- Shen DM, Jale SR, Bulow M, Ojo AF (1999) Sorption thermodynamics of nitrogen and oxygen on CaA zeolite. *Stud Surf Sci Catal* 125:667-674
- Shroll RM, Smith DE (1999) Molecular dynamics simulations in the grand canonical ensemble: Application to clay mineral swelling. *J Chem Phys* 111:9025-9033
- Silvi B, Bouaziz A, Darco P (1993) Pseudopotential periodic Hartree-Fock study of Mg<sub>2</sub>SiO<sub>4</sub> polymorphs: Olivine, modified spinel and spinel. *Phys Chem Miner* 20:333-340
- Skipper NT, Chang FC, Sposito G (1995a) Monte Carlo simulation of interlayer molecular structure in swelling clay minerals: 1. Methodology. *Clays Clay Miner* 43:285-293
- Skipper NT, Refson K, McConnell JDC (1991) Computer simulation of interlayer water in 2:1 clays. *J Chem Phys* 94:7434-7445
- Skipper NT, Sposito G, Chang FC (1995b) Monte Carlo simulation of interlayer molecular structure in swelling clay minerals: 2. Monolayer hydrates. *Clays Clay Miner* 43:294-303
- Smit B (1995) Simulating the adsorption isotherms of methane, ethane, and propane in the zeolite silicalite. *J Phys Chem* 99:5597-5603
- Smit B, Siepmann JI (1994) Simulating the adsorption of alkanes in zeolites. *Science* 264:1118-1120
- Smith DE (1998) Molecular computer simulations of the swelling properties and interlayer structure of cesium montmorillonite. *Langmuir* 14:5959-5967

- Souda R, Yamamoto K, Hayami W, Aizawa T, Ishizawa Y (1994) Bond ionicity of alkaline earth oxides studied by low-energy D<sup>+</sup> scattering. *Phys Rev B: Condens Matter* 50:4733-4738
- Spasojevicde-Bire A, Kiat JM (1997) Electron deformation density studies of perovskite compounds. *Ferroelectrics* 199:143-158
- Sposito G, Park SH, Sutton R (1999) Monte Carlo simulation of the total radial distribution function for interlayer water in sodium and potassium montmorillonites. *Clays Clay Miner* 47:192-200
- Springborg M (1997) *Density-Functional Methods in Chemistry and Materials Science*. John Wiley and Sons, Chichester
- Stein DJ, Spera FJ (1995) Molecular dynamics simulations of liquids and glasses in the system NaAlSiO<sub>4</sub>-SiO<sub>2</sub>: Methodology and melt structures. *Am Mineral* 80:417-431
- Stixrude L, Cohen RE, Hemley RJ (1998) Theory of minerals at high pressure. *Rev Mineral* 37:639-671
- Stockman HW, Li CH, Wilson JL (1997) A lattice-gas and lattice Boltzmann study of mixing at continuous fracture junctions: Importance of boundary conditions. *Geophys Res Lett* 24:1515-1518
- Suzuki S, Takaba H, Yamaguchi T, Nakao S (2000) Estimation of gas permeability of a zeolite membrane based on a molecular simulation technique and permeation model. *J Phys Chem B* 104:1971-1976
- Teppen BJ, Rasmussen K, Bertsch PM, Miller DM, Schafer L (1997) Molecular dynamics modeling of clay minerals. 1. Gibbsite, kaolinite, pyrophyllite, and beidellite. *J Phys Chem B* 101:1579-1587
- Teppen BJ, Yu C, Miller DM, Schafer L (1998) Molecular dynamics simulations of sorption of organic compounds at the clay mineral / aqueous solution interface. *J Comput Chem* 19:144-153
- Terakura K, Yamasaki T, Uda T, Stich I (1997) Atomic and molecular processes on Si(001) and Si(111) surfaces. *Surf Sci* 386:207-215
- Teter DM (2000) Accurate and transferable ionic potentials from density functional theory. *Phys Rev Lett*:submitted
- Teter DM, Gibbs GV, Boisen MB, Allan DC, Teter MP (1995) First-principles study of several hypothetical silica framework structures. *Phys Rev B: Condens Matter* 52:8064-8073
- Teter MP, Payne MC, Allan DC (1989) Solution of Schrödinger equation for large systems. *Phys Rev B: Condens Matter* 40:12255-12263
- Tosi MP (1964) Cohesion of ionic solids in the Born model. *Solid State Phys* 131:533-545
- Tossell JA, Gibbs GV (1977) Molecular orbital studies of geometries and spectra of minerals and inorganic compounds. *Phys Chem Miner* 2:21-57
- Tossell JA, Gibbs GV (1978) The use of molecular-orbital calculations on model systems for the prediction of bridging-bond-angle variations in siloxanes, silicates, silicon nitrides and silicon sulfides. *Acta Crystallogr, Sect A: Found Crystallogr* 34:463-472
- Tossell JA, Vaughan DJ (1992) *Theoretical Geochemistry: Applications of Quantum Mechanics in the Earth and Mineral Sciences*. Oxford University Press, New York
- Tuckerman ME, Martyna GJ (2000) Understanding modern molecular dynamics: Techniques and applications. *J Phys Chem B* 104:159-178
- van't Hoff JH (1874) A suggestion looking to the extension into space of the structural formulas at present used in chemistry, and a note upon the relation between the optical activity and the chemical constitution of organic compounds. *Arch Neerland Sci Exact Natur* 9:445-454
- Verlet L (1967) Computer 'experiments' on classical fluids: I. Therodynamical properties of Lennard-Jones molecules. *Phys Rev* 159:98-103
- Wallace DC (1972) *Thermodynamics of Crystals*. Dover Publications, Mineola, New York
- Wang J, Kalinichev AG, Kirkpatrick RJ, Hou X (2001) Molecular modeling of the structure and energetics of hydrotalcite hydration. *Chem Mater* 13:145-150
- Watson GW, Oliver PM, Parker SC (1997) Computer simulation of the structure and stability of forsterite surfaces. *Phys Chem Miner* 25:70-78
- Wentzcovitch RM, Martins JL, Price GD (1993) *Ab initio* molecular dynamics with variable cell shape: Application to MgSiO<sub>3</sub>. *Phys Rev Lett* 70:3947-3950
- Wentzcovitch RM, Stixrude L (1997) Crystal chemistry of forsterite: A first-principles study. *Am Mineral* 82:663-671
- Winkler B, Blaha P, Schwarz K (1996) *Ab initio* calculation of electric-field-gradient tensors of forsterite. *Am Mineral* 81:545-549
- Winkler B, Dove MT (1992) Thermodynamic properties of MgSiO<sub>3</sub> perovskite derived from large-scale molecular dynamics simulations. *Phys Chem Miner* 18:407-415
- Woodcock LV, Angell CA, Cheeseman P (1976) Molecular dynamics studies of the vitreous state: Simple ionic systems and silica. *J Chem Phys* 65:1565-1577
- Zhang HY, Bukowinski MST (1991) Modified potential-induced breathing model of potentials between closed-shell ions. *Phys Rev B: Condens Matter* 44:2495-2503